Special Issue - Igor Sevostianov Special Issue of the journal of Mathematics and Mechanics of Solids

MMS

Mathematics and Mechanics of Solids
1–33

DOI: 10.1177/10812865221136269
journals.sagepub.com/home/mms
SAGE

Asymptotic homogenization of flexoelectric composite plates with periodically varying thickness

AL Kalamkarov
Department of Mechanical Engineering, Dalhousie University, Halifax, NS, Canada

DA Hadjiloizi
Bernal Institute, University of Limerick, Limerick, Ireland

PM Weaver
Bernal Institute, University of Limerick, Limerick, Ireland

AV Georgiades
Department of Mechanical Engineering and Materials Science and Engineering, Cyprus University of Technology, Limassol, Cyprus; Research Unit for Nanostructured Materials Systems, Department of Mechanical Engineering and Materials Science and Engineering, Cyprus University of Technology, Limassol, Cyprus

Received 22 April 2022; accepted 14 October 2022

Abstract
A micromechanical model for the analysis of structurally periodic flexoelectric plates with periodically varying thickness is developed on the basis of asymptotic homogenization. The period of thickness variation is small and comparable to the plate thickness; accordingly, the plate is usually referred to as having a "rapidly varying thickness." The stipulation for rapidly varying thickness is important because it is envisioned that the developed model can be applied to a broad range of thin plates, both stratified as well as plates endowed with an arbitrary distribution of reinforcements attached to the surface or embedded within the plate. The microscopic problem is implemented in two steps pertaining, respectively, to first- and second-gradient asymptotic homogenization. Each level of homogenization culminates in its own set of unit cell problems from which the effective coefficients of the homogenized structure can eventually be obtained. These effective coefficients couple the force and moment resultants as well as the averaged electric displacement with the first and second gradients of the macroscopic displacement and electric potential. Once the effective coefficients are obtained, the

Corresponding authors:
AL Kalamkarov, Department of Mechanical Engineering, Dalhousie University, PO Box 15000, Halifax, NS B3H 4R2, Canada.
Email: Alex.Kalamkarov@dal.ca

AV Georgiades, Department of Mechanical Engineering and Materials Science and Engineering, Cyprus University of Technology, Limassol, 3041, Cyprus.
Email: Tasos.Georgiades@cut.ac.cy

macroscopic problem is invoked, which provides a set of four differential equations from which the macroscopic variables of mechanical displacement and electric potential can be obtained. The model is illustrated by means of laminated flexoelectric composites as well as simple rib-reinforced plates. It is shown that in the limiting case of a thin, purely elastic plate, the derived model converges to the familiar classical plate model.

Keywords
Flexoelectric Plates, first- and second-gradient asymptotic homogenization, effective properties, reinforced plates

1. Introduction

A major issue in micromechanics of advanced composite materials is determination of the effective properties of highly inhomogeneous composites, which will naturally depend on the spatial distribution, geometric characteristics, and mechanical properties of the constituent materials of the composite. At present, different methods have been developed and applied to the micromechanical analysis of composite materials. A highly significant contribution regarding the quantitative characterization of microstructure of composites, calculation of their effective properties, microstructure-properties relationships, and cross-property connections was made by Igor Sevostianov, see, e.g., Sevostianov [1], Sevostianov and Kachanov [2–4], and Sevostianov and Giraud [5].

Recent developments in micro/nano electromechanical systems (MEMSs/NEMSs) and devices have spurred the exponential growth of the nanotechnology sector. At the forefront of these developments are devices that exploit the coupling between electrical and mechanical energy such as nanomotors, nanomachines and nanorobots [6], piezotronic transistors and piezotronics [7], nanoelectromechanical switches [8], sensors and actuators [9,10], and many other devices and systems [11]. The physical property that is predominantly used to transduce electrical to mechanical energy is piezoelectricity which describes the generation of electric polarization in response to an applied uniform mechanical strain, or, conversely, the induction of mechanical deformation under the application of an electric field. However, since piezoelectricity is mathematically described by a third-order tensor, it must vanish (as must all odd-order tensors) under inversion-center symmetry; as a result, piezoelectricity is restricted to non-centrosymmetric crystals and many common dielectric materials do not exhibit piezoelectricity [12]. The presence of non-uniform strain however, or, equivalently, strain gradient, can override the crystallographic symmetry of centrosymmetric crystals so that they, too, can undergo polarization. An excellent physical description of this phenomenon can be found in Maranganti et al. [12] and Sharma et al. [13, 14]. This induction of polarization response under an applied mechanical strain gradient is called direct flexoelectricity, and the mechanical deformation response under an applied electric field gradient is called converse flexoelectricity, see for example, Maranganti et al. [12], Sharma et al. [13,14], Shu et al. [15], and Huang et al. [16]. Even though from a theoretical perspective at least, all dielectric materials exhibit flexoelectricity, this phenomenon is negligible at the micron or mm scales where the strain and field gradients are, ordinarily, small. However, since these gradients scale inversely with size, then one can appreciate that flexoelectric coupling becomes more prominent at the nanoscale and can be exploited for many emerging nanotechnology applications [15–19] provided that the pertinent nanostructures are properly designed [13]. For comprehensive review works on different aspects of flexoelectricity, the reader is referred to the works of Yudin and Tagantsev [19], Shu et al. [15], Huang et al. [16], and many others.

Clearly, the incorporation of flexoelectric components, devices, and systems in new engineering applications will be facilitated if their properties are known at the design stage; thus, micro/nano mechanical models become important. The pioneering contributions with respect to gradient effects are attributed to the nonlocal theory developed by Mindlin [20] who formulated a comprehensive linear model for the deformation of an elastic body based on the functional dependence of the potential energy density on both strain as well as its first and second gradients. Since then, and more systematically in recent years, a significant volume of associated works has been disseminated in the literature pertaining to various modeling aspects such as topology optimization of multimaterial flexoelectric composites [21–23], numerical and/or analytical determination of the effective properties of flexoelectric structures [24–29], bending and vibration analysis of flexoelectric beams [30–33], dynamic analysis and control of flexoelectric plates

and shells [34–38], and many others. Ever since the rapid growth of the additive manufacturing industry has significantly facilitated fabrication of composites and metamaterials with arbitrary architectures, it stands to reason that the development of models that predict their behavior and properties a priori is a step in the right direction. Furthermore, since thin-walled structures (beams, plates, and shells) constitute significant elements of emerging MEMS/NEMS devices and systems, our objective in this work is to develop a comprehensive micromechanical model pertaining to flexoelectric plates with periodically varying thickness. The period of thickness variation is small and comparable to the plate thickness; accordingly, and in the language of asymptotic homogenization, the plate is usually referred to as having a "rapidly varying thickness." The "rapidly varying thickness" stipulation is important in that it will broaden the applicability of the model to not only laminated structures but also flexoelectric reinforced plates endowed with an arbitrary arrangement of reinforcements and/or actuators bonded to the top and bottom surface (or embedded within the plate). In other words, the periodic distribution of reinforcing elements (e.g., ribs or spars) or sensors/actuators (e.g., piezoelectric) on the top and bottom surfaces will give the plate a "rapidly varying thickness" and, at the same time, widen the range of structures that can be designed and analyzed. To the best of our knowledge, there is a relative shortage of such reported models and we hope that current work will constitute a welcome addition to the existing literature. We note here some of our recent works where we followed this strategy for magnetoelectric composite and reinforced plates and shells [39–44], albeit using only first-gradient homogenization.

Since most advanced composites and metamaterials currently being modeled, designed, and fabricated have a periodic or nearly periodic configuration, they lend themselves nicely to analytic treatment via the method of asymptotic homogenization. The relevant mathematical details can be found in Bensoussan et al. [45], Sanchez-Palencia [46], Bakhvalov and Panasenko [47], and Cioranescu and Donato [48]. Briefly, when analyzing an advanced composite structure, one has to deal with two sources of complication; coupling between two spatial scales, the microscopic and macroscopic scales, and physical coupling between different fields such as mechanical, electrical, magnetic, thermal, and so on. The overarching characteristic of asymptotic homogenization is that it successfully decouples the microscopic and the macroscopic scales so that the two can be treated separately. The microscopic scale governs the substructural characteristics of the composite because of the different constituents and their relative spatial configuration and physical behavior while the macroscopic scale is a manifestation of the global formulation of the problem. Central to the microscopic scale is the recovery of the so-called unit cell problems, solved entirely in the domain of a periodicity or unit cell, which eventually permit the determination of the effective coefficients. Once determined, these effective coefficients are universal in nature and can be used to analyze a broad range of boundary value problems associated with the given geometrical setting. The effective coefficients then enter the governing equations of the homogenized structure formulated in terms of a set of macroscopic variables that may be calculated. In the model we are developing in this work, these latter variables are the three components of mechanical displacement and the electric potential. Once these are determined, the relevant field variables (stress, strain, electric displacement, etc.) are obtained in terms of the first and second gradients of mechanical displacement and electric potential (or, equivalently strain, strain gradient, electric field, and field gradient). This is the macroscopic problem.

Many problems in elasticity, electro/magnetoelasticity, and thermoelasticity have been solved on the basis of asymptotic homogenization. Kalamkarov et al. [49] and Kalamkarov and Kolpakov [50] examined a broad range of problems related to the modeling and design of composite plates and shells. Hadjiloizi et al. [51] developed a quasi-static asymptotic homogenization model pertaining to magnetoelectric thin plates with rapidly varying thickness and obtained closed-form expressions for the effective properties of stratified structures as well as rib- and wafer-reinforced plates. Important among the effective properties are the so-called product properties, the most common of which are magnetoelectricity, pyroelectricity, and pyromagnetism. These are properties that develop when piezoelectric and piezomagnetic constituents are present in a composite structure but are not typically exhibited by either piezoelectric or piezomagnetic materials on their own. In an interesting application of this work concerning elastic aerospace applications, Hadjiloizi et al. [52] obtained closed-form expressions for the effective properties of wingbox structures with trapezoidally arranged reinforcements. In addition to the aforementioned quasi-static models, Hadjiloizi et al. [53–55] formulated dynamic models for magnetoelectric plates and shells wherein it was shown that the homogenized structures exhibited memory-like behavior

even though none of the constituents were taken to be viscoelastic to begin with Christofi et al. [44]. Guinovart-Sanjuán et al. [56–59] developed comprehensive micromechanical models for thick laminated shells with perfect and non-perfect interface bonding. Interesting applications of their work include laminated shells with complex geometrical architecture such as chevron-like structures as well as thick laminated shells with non-constant thickness.

Other state-of-the art research activities that showcase the application or potential for application of asymptotic homogenization and variational asymptotic homogenization pertain to bi-pantographic fabrics, biological materials, bio-inspired implants, three-dimensional cellular structures and general topologically and geometrically interlocked architecture materials [60–62], hierarchical infills for additive manufacturing [29,63,64], piezoelectric nanogenerators for flexible electronics [65], wave propagation in periodic viscoelastic materials [66], thermoelastic materials with spatially dependent periodic relaxation time [67], thin films/nanostructures including surface and interface properties [68], and many others. Many of these emerging classes of materials cannot, usually, be adequately analyzed using first-gradient homogenization and their modeling inevitably invokes second-gradient effects. In turn, this necessitates an expanded set of effective properties that must be determined from the analysis.

Motivated by the foregoing applications, our objective is to develop a general first- and second-order asymptotic homogenization model for thin flexoelectric plates with rapidly varying thickness. Most of the published works using higher-order asymptotic homogenization essentially use a three-dimensional formalism with periodicity in all directions. Instead, our interest lies in analyzing composite plate structures with distinct in-plane and out-of-plane behavior (such as bending and torsion) whereby periodicity exists only in the tangential directions but not in the transverse direction. Furthermore, we are interested in a model that is applicable to both laminated structures and reinforced flexoelectric plates endowed with an arbitrary arrangement of reinforcements and/or actuators attached to the top and bottom surface of the plate or embedded within the plate.

Following this Introduction, the remainder of the paper is organized as follows: Sections 2 and 3 set up the problem and define the relevant variables. The associated asymptotic homogenization problem is derived in Sections 4 (involving first gradient of mechanical displacement and electric potential) and 5 (second-order homogenization) and include the unit cell problems with their boundary conditions. Section 6 describes the macroscopic problem, obtains expressions for the effective coefficients, and compares limiting cases of the model with previously published results. Section 7 illustrates application of the model to thin laminates and a ribbed plate and, finally, Section 8 concludes the work.

2. Fundamental expressions and variables

The electrical enthalpy density, $\Im$, of a flexoelectric dielectric material may be written in terms of the mechanical strain, electric field as well as their gradients, see Sharma [14], Hu and Shen [69], Shen and Hu [70], Zhuang [71], and Abdollahi et al. [72] as,

$$\begin{aligned}\Im\left(\varepsilon_{ij},\varepsilon_{ij,k},E_i,E_{i,k}\right)=&\frac{1}{2}C_{ijkl}\varepsilon_{ij}\varepsilon_{kl}-e_{ikl}E_i\varepsilon_{kl}+\mu_{lijk}\varepsilon_{ij}E_{l,k}-\mu_{ijkl}E_i\varepsilon_{jk,l}-\frac{1}{2}\kappa_{ij}E_iE_j+\\&-\frac{1}{2}b_{ijkl}E_{i,j}E_{k,l}+h_{ijk}E_iE_{j,k}+r_{ijklm}\varepsilon_{ij}\varepsilon_{kl,m}+\eta_{ijklm}E_{i,j}\varepsilon_{kl,m}+\frac{1}{2}g_{ijklmn}\varepsilon_{ij,k}\varepsilon_{lm,n}.\end{aligned}\tag{2.1}$$

Here, ε_{ij} and $\varepsilon_{ij,k}$ are the mechanical strain and strain gradient; E_i and $E_{i,k}$ the electric field and its gradient; e_{ikl}, κ_{ij}, μ_{ijkl} the piezoelectric, dielectric permittivity and flexoelectric tensors; h_{ijk}, b_{ijkl}, η_{ijklm} are higher-order tensors coupling the field gradient to the electric displacement, higher-order electric displacement, and higher-order mechanical stress (to be defined shortly), respectively; and, finally, r_{ijklm}, g_{ijklmn} are higher-order elasticity tensors coupling the strain gradient to stress and higher-order stress. We also assume that the electric field may be expressed as the gradient of a scalar function φ as,

$$E_i=-\varphi_{,i}.\tag{2.2a}$$

The mechanical strain (linearized Green-Lagrange strain tensor) is defined in terms of the mechanical displacement, u_i, as,

$$\varepsilon_{ij} = \frac{1}{2}\left(u_{i,j} + u_{j,i}\right), \tag{2.2b}$$

while the strain gradient and field gradient will, henceforth, be denoted by ω_{ijk} and V_{ij}, respectively. Thus,

$$\omega_{ijk} = \varepsilon_{ij,k}, \quad V_{ij} = E_{i,j}. \tag{2.2c}$$

Equation (2.1) can be used to obtain the constitutive relationships for stress, σ_{ij}, higher-order stress, τ_{ijk}, electric displacement, D_i and higher-order electric displacement, D_{ij}, see Zhuang et al. [71], Abdollahi et al. [72], according to,

$$\begin{aligned}
\sigma_{ij} &= \frac{\partial \Im}{\partial \varepsilon_{ij}} = C_{ijkl}\varepsilon_{kl} - e_{kij}E_k + \mu_{lijk}V_{lk} + r_{ijklm}\omega_{klm} \\
D_i &= -\frac{\partial \Im}{\partial E_i} = e_{ikl}\varepsilon_{kl} + \kappa_{ij}E_j + \mu_{ijkl}\omega_{jkl} - h_{ijk}V_{jk} \\
\tau_{ijk} &= \frac{\partial \Im}{\partial \omega_{ijk}} = -\mu_{lijk}E_l + r_{lmijk}\varepsilon_{lm} + \eta_{lmijk}V_{lm} + g_{ijklmn}\omega_{klm} \\
D_{ij} &= -\frac{\partial \Im}{\partial V_{ij}} = -\mu_{iklj}\varepsilon_{kl} + b_{ijkl}V_{kl} - h_{kij}E_k - \eta_{ijklm}\omega_{klm}.
\end{aligned} \tag{2.3}$$

It should be noted that in many works, distinction is made between the direct and converse flexoelectric tensors (as noted in the previous section). However, as detailed in Sharma et al. [14], one can express the electric enthalpy in terms of only one of these tensors, see also Guinovart-Sanjuán [24], Zhuang et al. [71], and we also chose to do so in equation (2.1). In parallel with Abdollahi et al. [72], one may also define the "physical" stress, σ^*_{ij}, and "physical" electric displacement, D^*_i, as follows:

$$\sigma^*_{ij} = \sigma_{ij} - \tau_{ijk,k} \qquad D^*_i = D_i - D_{ij,j}. \tag{2.4}$$

Next, defining the total electrical enthalpy as in Abdollahi et al. [72], and applying the virtual work principle yields the pertinent equilibrium equations in the form of,

$$\begin{aligned}
\left(\sigma_{ij} - \tau_{ijk,k}\right)_{,j} + P_i = 0 \qquad &or \qquad \sigma^*_{ij,j} + P_i = 0 \\
\left(D_j - D_{jk,k}\right)_{,j} - \rho^* = 0 \qquad &or \qquad D^*_{j,j} - \rho^* = 0.
\end{aligned} \tag{2.5a}$$

Finally, the boundary conditions may be taken as follows:

$$\begin{aligned}
\left(\sigma_{ij} - \tau_{ijk,k}\right)n_j = p_i \qquad &or \qquad \sigma^*_{ij}n_j = p_i \\
\left(D_j - D_{jk,k}\right)n_j = -\sigma^* \qquad &or \qquad D^*_j n_j = -\sigma^*.
\end{aligned} \tag{2.5b}$$

Here, n_i is the normal vector; P_i and ρ^* are the body force and charge density, respectively; while p_i and σ^* stand for the surface traction and surface charge density. It is worth noting that more complicated forms for the equilibrium equations and boundary conditions may be derived from application of virtual work, as detailed, for example, in Hu and Shen [69] and Zhuang [71]. However, equations (2.5a) and (2.5b) will suffice for our purpose.

3. Simplified problem formulation

Consider a thin flexoelectric and piezoelectric layer representing an inhomogeneous solid with wavy surfaces as shown in Figure 1. This periodic structure is generated by repeating the so-called periodicity cell or unit cell in the $x_1 - x_2$ plane, and it is assumed that all three coordinates are made dimensionless by

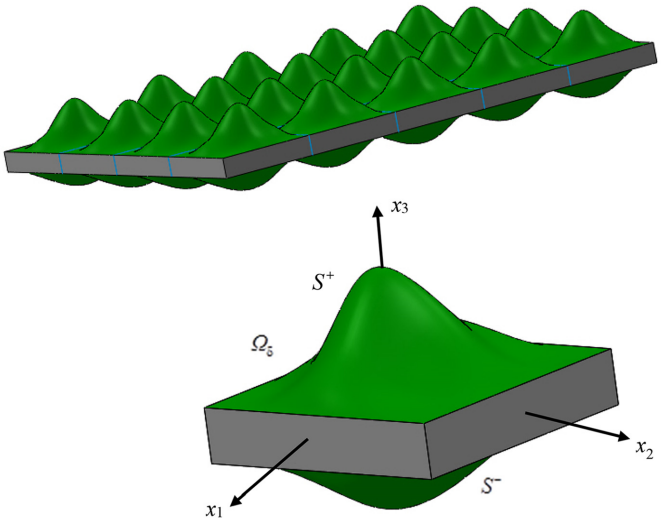

Figure 1. Periodic piezoelectric and flexoelectric layer and its periodicity (unit) cell.

dividing by a certain characteristic dimension of the body. The "waviness" of the top and bottom surfaces models an arbitrary motif as dictated by the type and spatial orientation of reinforcements and/or actuators attached to these surfaces. Clearly, the absence of any surface reinforcements gives rise to a constant thickness flexoelectric plate. It is also assumed that a periodic arrangement of reinforcements or actuators may also, or instead, be embedded inside the thin-walled structure.

The unit cell of the problem is defined by the following inequalities (see Figure 1):

$$\left\{-\frac{\delta h_1}{2}<x_1<\frac{\delta h_1}{2},\quad -\frac{\delta h_2}{2}<x_2<\frac{\delta h_2}{2},\quad S^-<x_3<S^+\right\},\quad \text{where}$$
$$S^\pm=\pm\frac{\delta}{2}\pm\delta F^\pm\left(\frac{x_1}{\delta h_1},\frac{x_2}{\delta h_2}\right). \tag{3.1}$$

Here, h_1 and h_2 define the tangential dimensions of the unit cell and $F^\pm$ defines the profile of the top/bottom surfaces.

To reduce the complexity of the resulting expressions, we choose to ignore the higher-order stress and electric displacement as well as the associated material tensors with the exception of the flexoelectric tensor. Thus, the equilibrium equations governing the composite of Figure 1 reduce from those in equation (2.5b) to,

$$\frac{\partial\sigma_{ij}\left(x_i,\frac{x_\alpha}{\delta h_\alpha}\right)}{\partial x_j}+P_i\left(x_i,\frac{x_\alpha}{\delta h_\alpha}\right)=0;\qquad \frac{\partial D_j\left(x_i,\frac{x_\alpha}{\delta h_\alpha}\right)}{\partial x_j}-\rho^*\left(x_i,\frac{x_\alpha}{\delta h_\alpha}\right)=0. \tag{3.2a}$$

In equation (3.2a) and in the sequel, we make use of the frequently adopted convention whereby Latin indices $i, j, k, \ldots$ assume values of 1, 2, and 3 while their Greek counterparts, $\alpha, \beta, \gamma, \ldots$ take on values of 1 or 2 only. The functional dependence of the involved field variables in equation (3.2a) points to the periodicity in the tangential directions (1, 2) only but not in the transverse direction. As we will see later on, this has important ramifications in the form of the unit cell problems to be derived, in that they will be endowed with boundary conditions on the top and bottom surfaces (reflecting the absence of periodicity in the x_3 direction) as opposed to "classical" unit cell problems, see, for example, Bakhvalov and Panasenko [47].

The boundary conditions on the top and bottom surfaces of the flexoelectric composite reduce from those in equation (2.5b) to,

$$\sigma_{ij}^{\pm} n_j^{\pm} = p_i^{\pm} \qquad \text{and} \qquad D_j^{\pm} n_j^{\pm} = -\sigma^{*\pm} \qquad \text{on } S^{\pm}, \tag{3.2b}$$

where $n_j^{+}(n_j^{-})$ is the outward (inward) unit normal vector on the top (bottom) surfaces given by,

$$\mathbf{n}^{\pm} = \left(\mp \frac{\partial S^{\pm}}{\partial x_1}, \mp \frac{\partial S^{\pm}}{\partial x_2}, 1 \right) \left[\left(\frac{\partial S^{\pm}}{\partial x_1} \right)^2 + \left(\frac{\partial S^{\pm}}{\partial x_2} \right)^2 + 1 \right]^{-\frac{1}{2}}. \tag{3.2c}$$

We also assume the following conditions on the tangential surfaces,

$$u_i = 0, \quad \varphi = \delta \lambda_1 + \delta^2 \lambda_2, \tag{3.2d}$$

where λ_1 and λ_2 are potential functions.

Furthermore, the relevant constitutive equations become,

$$\sigma_{ij} = C_{ijkl} \varepsilon_{kl} - e_{kij} E_k + \mu_{lijk} V_{lk}, \qquad D_i = e_{ikl} \varepsilon_{kl} + \kappa_{ij} E_j + \mu_{ijkl} \omega_{jkl}. \tag{3.2e}$$

It can be readily deduced from equations (2.3) or (3.2e) that the flexoelectric coefficients are symmetric with respect to the middle two indices, see Guinovart-Sanjuán et al. [24,25].

Microscopic analysis begins by the introduction of the so-called "fast" variables according to,

$$y_1 = \frac{x_1}{\delta h_1}, \quad y_2 = \frac{x_1}{\delta h_2}, \quad z = \frac{x_3}{\delta}, \tag{3.3}$$

so that the unit cell Ω_δ is defined by,

$$\begin{aligned} &\{-1/2 < y_1 < 1/2, \quad -1/2 < y_2 < 1/2, \quad Z^- < z < Z^+\}, \quad \text{with} \quad Z^{\pm} = \pm \frac{1}{2} \pm F^{\pm}(\mathbf{y}) \\ &\text{and} \quad \mathbf{y} = (y_1, y_2), \quad \mathbf{x} = (x_1, x_2), \end{aligned} \tag{3.4}$$

and the unit normal vector from equation (3.2c) becomes,

$$\mathbf{n}^{\pm} = \left(\mp \frac{1}{h_1} \frac{\partial F^{\pm}}{\partial y_1}, \mp \frac{1}{h_2} \frac{\partial F^{\pm}}{\partial y_2}, 1 \right) \left[1 + \frac{1}{h_1^2} \left(\frac{\partial F^{\pm}}{\partial y_1} \right)^2 + \frac{1}{h_2^2} \left(\frac{\partial F^{\pm}}{\partial y_2} \right)^2 \right]^{-\frac{1}{2}}. \tag{3.5}$$

The introduction of the microscopic variables, y_α, z, necessitates the transformation of the derivatives according to,

$$\frac{\partial}{\partial x_\alpha} \to \frac{\partial}{\partial x_\alpha} + \frac{1}{\delta h_\alpha} \frac{\partial}{\partial y_\alpha} \quad \text{and} \quad \frac{\partial}{\partial x_3} = \frac{1}{\delta} \frac{\partial}{\partial z}, \tag{3.6a}$$

and from here onward, we adopt the following compact notations with respect to derivatives:

$$\begin{aligned} &\frac{\partial(\ldots)}{\partial x_\alpha} = (\ldots)_{,\alpha} \; ; \; \frac{\partial(\ldots)}{\partial y_\alpha} = (\ldots)_{|\alpha} \; ; \; \frac{\partial(\ldots)}{\partial z} = (\ldots)_{|3} \; ; \; \frac{\partial^2(\ldots)}{\partial x_\alpha x_b} = (\ldots)_{,\alpha\beta} \; ; \; \frac{\partial^2(\ldots)}{\partial y_\alpha y_b} = (\ldots)_{|\alpha\beta} \\ &\frac{\partial^2(\ldots)}{\partial y_\alpha \partial x_\beta} = \frac{\partial}{\partial y_\alpha}(\ldots)_{,\beta} \; ; \; \frac{\partial^2(\ldots)}{\partial z \partial x_\beta} = \frac{\partial}{\partial z}(\ldots)_{,\beta} \; ; \; \frac{\partial^2(\ldots)}{\partial z^2} = (\ldots)_{|33}. \end{aligned} \tag{3.6b}$$

Furthermore, we make the following asymptotic assumptions:

$$p_\alpha^{\pm} = \delta^3 r_\alpha^{*\pm}, \quad p_3^{\pm} = \delta^4 q_3^{*\pm}, \quad P_\alpha = \delta^2 f_\alpha^*, \quad P_3 = \delta^3 g_3^*, \quad \sigma^{*\pm} = \delta^3 \hat{\sigma}, \quad \rho^* = \delta^2 \hat{\rho}, \tag{3.7a}$$

and

$$\mu_{lijk} = \delta \mu^{(f)}_{lijk}. \tag{3.7b}$$

The next step in the analysis involves the asymptotic expansion of each field variable in terms of powers of δ as follows:

$$\begin{aligned}
u_i(\boldsymbol{x},\boldsymbol{y},z) &= u_i^{(0)}(\boldsymbol{x},\boldsymbol{y},z) + \delta u_i^{(1)}(\boldsymbol{x},\boldsymbol{y},z) + \delta^2 u_i^{(2)}(\boldsymbol{x},\boldsymbol{y},z) + \ldots \\
\varepsilon_{ij}(\boldsymbol{x},\boldsymbol{y},z) &= \varepsilon_{ij}^{(0)}(\boldsymbol{x},\boldsymbol{y},z) + \delta \varepsilon_{ij}^{(1)}(\boldsymbol{x},\boldsymbol{y},z) + \delta^2 \varepsilon_{ij}^{(2)}(\boldsymbol{x},\boldsymbol{y},z) + \ldots \\
\omega_{ijk}(\boldsymbol{x},\boldsymbol{y},z) &= \omega_{ijk}^{(0)}(\boldsymbol{x},\boldsymbol{y},z) + \delta \omega_{ijk}^{(1)}(\boldsymbol{x},\boldsymbol{y},z) + \delta^2 \omega_{ijk}^{(2)}(\boldsymbol{x},\boldsymbol{y},z) + \ldots \\
\sigma_{ij}(\boldsymbol{x},\boldsymbol{y},z) &= \sigma_{ij}^{(0)}(\boldsymbol{x},\boldsymbol{y},z) + \delta \sigma_{ij}^{(1)}(\boldsymbol{x},\boldsymbol{y},z) + \delta^2 \sigma_{ij}^{(2)}(\boldsymbol{x},\boldsymbol{y},z) + \ldots
\end{aligned} \tag{3.8a}$$

$$\begin{aligned}
\varphi(\boldsymbol{x},\boldsymbol{y},z) &= \varphi^{(0)}(\boldsymbol{x},\boldsymbol{y},z) + \delta \varphi^{(1)}(\boldsymbol{x},\boldsymbol{y},z) + \delta^2 \varphi^{(2)}(\boldsymbol{x},\boldsymbol{y},z) + \ldots \\
E_i(\boldsymbol{x},\boldsymbol{y},z) &= E_i^{(0)}(\boldsymbol{x},\boldsymbol{y},z) + \delta E_i^{(1)}(\boldsymbol{x},\boldsymbol{y},z) + \delta^2 E_i^{(2)}(\boldsymbol{x},\boldsymbol{y},z) + \ldots \\
V_{ij}(\boldsymbol{x},\boldsymbol{y},z) &= V_{ij}^{(0)}(\boldsymbol{x},\boldsymbol{y},z) + \delta V_{ij}^{(1)}(\boldsymbol{x},\boldsymbol{y},z) + \delta^2 V_{ij}^{(2)}(\boldsymbol{x},\boldsymbol{y},z) + \ldots \\
D_i(\boldsymbol{x},\boldsymbol{y},z) &= D_i^{(0)}(\boldsymbol{x},\boldsymbol{y},z) + \delta D_i^{(1)}(\boldsymbol{x},\boldsymbol{y},z) + \delta^2 D_i^{(2)}(\boldsymbol{x},\boldsymbol{y},z) + \ldots
\end{aligned} \tag{3.8b}$$

We would like to express the mechanical strain and its gradient, the electric field and its gradient as well as the mechanical stress and electric displacement as functions of the mechanical displacement and electric potential. To this end, we make use of equations (2.2b), (2.2c), and (3.6a) to obtain for strain, strain gradient, and stress:

$$\begin{aligned}
\varepsilon^{(n)}_{\alpha\beta}(\boldsymbol{x},\boldsymbol{y},z) &= \frac{1}{2}\left(u^{(n)}_{\alpha,\beta} + u^{(n)}_{\beta,\alpha}\right) + \frac{1}{2}\left(\frac{1}{h_\beta}u^{(n+1)}_{\alpha|\beta} + \frac{1}{h_\alpha}u^{(n+1)}_{\beta|\alpha}\right) \\
\varepsilon^{(n)}_{3\beta} &= \frac{1}{2}\left(u^{(n)}_{3,\beta} + \frac{1}{h_\beta}u^{(n+1)}_{3|\beta} + u^{(n+1)}_{\beta|3}\right), \quad \varepsilon^{(n)}_{33} = u^{(n+1)}_{3|3}, \quad n = 0, 1, 2\ldots
\end{aligned} \tag{3.9a}$$

$$\begin{aligned}
\omega^{(n)}_{\alpha\beta\nu}(\boldsymbol{x},\boldsymbol{y},z) &= \frac{1}{2}\frac{\partial}{\partial x_\nu}\left(u^{(n)}_{\alpha,\beta} + u^{(n)}_{\beta,\alpha} + \frac{1}{h_\beta}u^{(n+1)}_{\alpha|\beta} + \frac{1}{h_\alpha}u^{(n+1)}_{\beta|\alpha}\right) + \\
&\quad + \frac{1}{2}\frac{1}{h_\nu}\frac{\partial}{\partial y_\nu}\left(u^{(n+1)}_{\alpha,\beta} + u^{(n+1)}_{\beta,\alpha} + \frac{1}{h_\beta}u^{(n+2)}_{\alpha|\beta} + \frac{1}{h_\alpha}u^{(n+2)}_{\beta|\alpha}\right) \\
\omega^{(n)}_{3\beta\nu} &= \frac{1}{2}\frac{\partial}{\partial x_\nu}\left(u^{(n)}_{3,\beta} + \frac{1}{h_\beta}u^{(n+1)}_{3|\beta} + u^{(n+1)}_{\beta|3}\right) + \frac{1}{2}\frac{1}{h_\nu}\frac{\partial}{\partial y_\nu}\left(u^{(n+1)}_{3,\beta} + \frac{1}{h_\beta}u^{(n+2)}_{3|\beta} + u^{(n+2)}_{\beta|3}\right) \\
\omega^{(n)}_{\alpha\beta3} &= \frac{1}{2}\frac{\partial}{\partial z}\left(u^{(n+1)}_{\alpha,\beta} + u^{(n+1)}_{\beta,\alpha} + \frac{1}{h_\beta}u^{(n+2)}_{\alpha|\beta} + \frac{1}{h_\alpha}u^{(n+2)}_{\beta|\alpha}\right), \quad \omega^{(n)}_{333} = \frac{\partial}{\partial z}\left(u^{(n+2)}_{3|3}\right) \\
\omega^{(n)}_{3\beta3} &= \frac{1}{2}\frac{\partial}{\partial z}\left(u^{(n+1)}_{3,\beta} + \frac{1}{h_\beta}u^{(n+2)}_{3|\beta} + u^{(n+2)}_{\beta|3}\right), \quad \omega^{(n)}_{33\nu} = \frac{\partial}{\partial x_\nu}\left(u^{(n+1)}_{3|3}\right) + \frac{1}{h_\nu}\frac{\partial}{\partial y_\nu}\left(u^{(n+2)}_{3|3}\right),
\end{aligned} \tag{3.9b}$$

$$\begin{aligned}
\sigma_{ij}^{(0)}(\boldsymbol{x},\boldsymbol{y},z) &= C_{ijk\beta}\left(u_{k,\beta}^{(0)}+\frac{1}{h_\beta}u_{k|\beta}^{(1)}\right)+C_{ijk3}u_{k|3}^{(1)}+e_{\beta ij}\left(\varphi_{,\beta}^{(0)}+\frac{1}{h_\beta}\varphi_{|\beta}^{(1)}\right)+e_{3ij}\varphi_{|3}^{(1)}\\
\sigma_{ij}^{(n)} &= C_{ijk\beta}\left(u_{k,\beta}^{(n)}+\frac{1}{h_\beta}u_{k|\beta}^{(n+1)}\right)+C_{ijk3}u_{k|3}^{(n+1)}+e_{\beta ij}\left(\varphi_{,\beta}^{(n)}+\frac{1}{h_\beta}\varphi_{|\beta}^{(n+1)}\right)+e_{3ij}\varphi_{|3}^{(n+1)}+\\
&-\mu_{\alpha ij\beta}^{(f)}\left(\varphi_{,\alpha\beta}^{(n-1)}+\frac{1}{h_\alpha}\frac{\partial}{\partial y_\alpha}\varphi_{,\beta}^{(n)}+\frac{1}{h_\beta}\frac{\partial}{\partial y_\beta}\varphi_{,\alpha}^{(n)}+\frac{1}{h_\alpha h_\beta}\varphi_{|\alpha\beta}^{(n+1)}\right)+\\
&-\left(\mu_{3ij\beta}^{(f)}+\mu_{\beta ij3}^{(f)}\right)\frac{\partial}{\partial z}\left(\varphi_{,\beta}^{(n)}+\frac{1}{h_\beta}\varphi_{|\beta}^{(n+1)}\right)-\mu_{3ij3}^{(f)}\left(\varphi_{|33}^{(n+1)}\right),\quad n\geqslant 1.
\end{aligned}\tag{3.9c}$$

Likewise, the corresponding expressions for the electric field, its gradient, and the electric displacement are obtained as follows:

$$E_\alpha^{(n)}(\boldsymbol{x},\boldsymbol{y},z)=-\varphi_{,\alpha}^{(n)}-\frac{1}{2}\frac{1}{h_\alpha}\varphi_{|\alpha}^{(n+1)},\qquad E_3^{(n)}(\boldsymbol{x},\boldsymbol{y},z)=-\varphi_{|3}^{(n+1)},\quad n=0,1,2...\tag{3.10a}$$

$$\begin{aligned}
V_{\alpha\beta}^{(n)}(\boldsymbol{x},\boldsymbol{y},z) &= -\frac{\partial}{\partial x_\beta}\left(\varphi_{,\alpha}^{(n)}+\frac{1}{h_\alpha}\varphi_{|\alpha}^{(n+1)}\right)-\frac{1}{h_\beta}\frac{\partial}{\partial y_\beta}\left(\varphi_{,\alpha}^{(n+1)}+\frac{1}{h_\alpha}\varphi_{|\alpha}^{(n+2)}\right)\\
V_{3\beta}^{(n)} &= -\frac{\partial}{\partial x_\beta}\left(\varphi_{|3}^{(n+1)}\right)-\frac{1}{h_\beta}\frac{\partial}{\partial y_\beta}\left(\varphi_{|3}^{(n+2)}\right),\quad V_{33}^{(n)}=-\varphi_{|33}^{(n+2)},\quad n=0,1,2...
\end{aligned}\tag{3.10b}$$

$$\begin{aligned}
D_i^{(0)}(\boldsymbol{x},\boldsymbol{y},z) &= e_{ik\beta}\left(u_{k,\beta}^{(0)}+\frac{1}{h_\beta}u_{k|\beta}^{(1)}\right)+e_{ik3}u_{k|3}^{(1)}-\kappa_{i\beta}\left(\varphi_{,\beta}^{(0)}+\frac{1}{h_\beta}\varphi_{|\beta}^{(1)}\right)-\kappa_{i3}\varphi_{|3}^{(1)}\\
D_i^{(n)} &= e_{ik\beta}\left(u_{k,\beta}^{(n)}+\frac{1}{h_\beta}u_{k|\beta}^{(n+1)}\right)+e_{ik3}u_{k|3}^{(n+1)}-\kappa_{i\beta}\left(\varphi_{,\beta}^{(n)}+\frac{1}{h_\beta}\varphi_{|\beta}^{(n+1)}\right)-\kappa_{i3}\varphi_{|3}^{(n+2)}+\\
&+\mu_{ik\alpha\beta}^{(f)}\left(u_{,\alpha\beta}^{(n-1)}+\frac{1}{h_\alpha}\frac{\partial}{\partial y_\alpha}u_{k,\beta}^{(n)}+\frac{1}{h_\beta}\frac{\partial}{\partial y_\beta}u_{k,\alpha}^{(n)}+\frac{1}{h_\alpha h_\beta}u_{k|\alpha\beta}^{(n+1)}\right)+\\
&+\left(\mu_{ik3\alpha}^{(f)}+\mu_{ik\alpha 3}^{(f)}\right)\frac{\partial}{\partial z}\left(u_{k,\alpha}^{(n)}+\frac{1}{h_\alpha}\frac{\partial}{\partial y_\alpha}u_{k|\alpha}^{(n+1)}\right)+\mu_{i3k3}^{(f)}\left(\varphi_{|33}^{(n+1)}\right),\quad n\geqslant 1.
\end{aligned}\tag{3.10c}$$

In the process of establishing (3.9a)–(3.10c), it is readily observed that the leading terms of the asymptotic expansions for mechanical displacement and strain, as well as electric potential and electric field are independent of the macroscopic variables so that we may write,

$$u_i^{(0)}=u_i^{(0)}(\boldsymbol{x}),\quad \varepsilon_{ij}^{(0)}=\varepsilon_{ij}^{(0)}(\boldsymbol{x}),\quad \varphi^{(0)}=\varphi^{(0)}(\boldsymbol{x}),\quad E_i^{(0)}=E_i^{(0)}(\boldsymbol{x}).\tag{3.11}$$

Before closing this section, let us introduce the averaging procedure:

$$\langle ...\rangle=\int_\Omega (...)dy_1dy_2dz.\tag{3.12}$$

Defined over the volume of the unit cell Ω and note an important result pertaining to an arbitrary function Q_i(periodic in y_1, y_2), which we will make frequent use of in the sequel:

$$\left\langle\frac{1}{h_\alpha}Q_{\alpha|\alpha}+Q_{3|3}\right\rangle=\int_{-1/2}^{1/2}\int_{-1/2}^{1/2}\left(Q_i^+N_i^+-Q_i^-N_i^-\right)dy_1dy_2.\tag{3.13}$$

Here, we make the following definition:

$$\boldsymbol{N}^\pm=\left(\mp\frac{1}{h_1}\frac{\partial F^\pm}{\partial y_1},\mp\frac{1}{h_2}\frac{\partial F^\pm}{\partial y_2},1\right).\tag{3.14}$$

The proof of equation (3.13) follows directly from application of the divergence theorem to the integral on the left-hand side (LHS) of equation (3.13) and imposing the periodicity of Q_i.

4. First-gradient homogenization

One of our main objectives in this work is to recover the unit cell problems from which the effective coefficients characterizing the homogenized flexoelectric solid can be determined. To this end, we substitute the asymptotic expansions for mechanical stress and electric displacement, equations (3.9c) and (3.10c), into the equilibrium equations and associated boundary conditions to obtain the following problems:

$$\begin{aligned}&\frac{1}{\delta}H_i^{(-1)}+H_i^{(0)}+\delta H_i^{(1)}+\delta^2 H_i^{(2)}+\cdots=0\\&\frac{1}{\delta}H^{*(-1)}+H^{*(0)}+\delta H^{*(1)}+\delta^2 H^{*(2)}+\cdots=0.\end{aligned}\tag{4.1a}$$

$$\begin{aligned}&\sigma_{ij}^{(0,1,2)}N_j^{\pm}=0,\quad \sigma_{ij}^{(3)}N_j^{\pm}=\pm\omega^{\pm}r_i^{*\pm}(\delta_{i1}+\delta_{i2}),\quad \sigma_{ij}^{(4)}N_j^{\pm}=\pm\omega^{\pm}q_i^{*\pm}(\delta_{i3})\\&D_i^{(0,1,2)}N_i^{\pm}=0,\quad D_i^{(3)}N_i^{\pm}=\pm\omega^{\pm}\hat{\sigma}^{\pm},\quad D_i^{(4)}N_i^{\pm}=0.\end{aligned}\tag{4.1b}$$

In equation (4.1a) we have,

$$\begin{aligned}&H_i^{(-1)}=\frac{1}{h_\beta}\sigma_{i\beta|\beta}^{(0)}+\sigma_{i3|3}^{(0)},\quad H_i^{(0,1)}=\sigma_{i\beta,\beta}^{(0,1)}+\frac{1}{h_\beta}\sigma_{i\beta|\beta}^{(1,2)}+\sigma_{i3|3}^{(1,2)}\\&H_i^{(2)}=\sigma_{i\beta,\beta}^{(2)}+\frac{1}{h_\beta}\sigma_{i\beta|\beta}^{(3)}+\sigma_{i3|3}^{(3)}+f_i^{*}(\delta_{i1}+\delta_{i2}),\quad H_i^{(3)}=\sigma_{i\beta,\beta}^{(3)}+\frac{1}{h_\beta}\sigma_{i\beta|\beta}^{(4)}+\sigma_{i3|3}^{(4)}+g_i^{*}(\delta_{i3}),\end{aligned}\tag{4.2a}$$

and

$$\begin{aligned}&H^{*(-1)}=\frac{1}{h_\beta}D_{\beta|\beta}^{(0)}+D_{3|3}^{(0)},\quad H^{*(0,1)}=D_{\beta,\beta}^{(0,1)}+\frac{1}{h_\beta}D_{\beta|\beta}^{(1,2)}+D_{3|3}^{(1,2)}\\&H^{*(2)}=D_{\beta,\beta}^{(2)}+\frac{1}{h_\beta}D_{\beta|\beta}^{(3)}+D_{3|3}^{(3)}-\hat{\rho},\quad H^{*(3)}=D_{\beta,\beta}^{(3)}+\frac{1}{h_\beta}D_{\beta|\beta}^{(4)}+D_{3|3}^{(4)}.\end{aligned}\tag{4.2b}$$

Furthermore, $\omega^{\pm}$ appearing in equation (4.1b) is defined as,

$$\omega^{\pm}=\sqrt{1+h_1^{-2}\left(F_{|1}^{\pm}\right)^2+h_2^{-2}\left(F_{|2}^{\pm}\right)^2}.\tag{4.3}$$

Since $H_i^{(-1)}=0$ and $H^{*(-1)}=0$ then, equations (4.1a) and (4.1b) yield the following boundary value problems:

$$\begin{array}{ll}\frac{1}{h_\beta}\sigma_{i\beta|\beta}^{(0)}+\sigma_{i3|3}^{(0)}=0 & \frac{1}{h_\beta}D_{\beta|\beta}^{(0)}+D_{3|3}^{(0)}=0\\ \sigma_{ij}^{(0)}N_j^{\pm}=0\quad \text{on } Z^{\pm} & D_i^{(0)}N_i^{\pm}=0\quad \text{on } Z^{\pm}\end{array}.\tag{4.4}$$

Substitution of $\sigma_{ij}^{(0)}$ and $D_i^{(0)}$ from equations (3.9c) and (3.10c) into equation (4.4) gives the following boundary value problems for $u_i^{(1)}$ and $\varphi^{(1)}$:

$$\begin{aligned}&D_{ik}u_k^{(1)}+C_i\varphi^{(1)}=-C_{ik\mu}(\boldsymbol{y},z)u_{k,\mu}^{(0)}(\boldsymbol{x})-P_{\mu i}(\boldsymbol{y},z)\varphi_{,\mu}^{(0)}(\boldsymbol{x})\\&\left[L_{ijk}u_k^{(1)}+M_{ij}\varphi^{(1)}+C_{ijk\mu}u_{k,\mu}^{(0)}+e_{\mu ij}\varphi_{,\mu}^{(0)}\right]N_j^{\pm}=0\quad\text{on}\quad Z^{\pm}.\end{aligned}\tag{4.5a}$$

$$\begin{aligned}&A_k^{*}u_k^{(1)}-L^{*}\varphi^{(1)}=-G_{k\mu}^{*}(\boldsymbol{y},z)u_{k,\mu}^{(0)}(\boldsymbol{x})+I_\mu^{*}(\boldsymbol{y},z)\varphi_{,\mu}^{(0)}(\boldsymbol{x})\\&\left[\Lambda_{ik}^{*}u_k^{(1)}-M_{ik}^{*}\varphi^{(1)}+e_{ik\mu}u_{k,\mu}^{(0)}-\kappa_{i\mu}\varphi_{,\mu}^{(0)}\right]N_j^{\pm}=0\quad\text{on}\quad Z^{\pm}.\end{aligned}\tag{4.5b}$$

The various differential operators appearing in equations (4.5a) and (4.5b) are defined in Appendix A. The separation of variables on the right-hand side (RHS) of equations (4.5a) and (4.5b) suggests a solution of the mechanical displacement and electric potential in the form of,

$$\begin{aligned} u_i^{(1)}(\boldsymbol{x},\boldsymbol{y},z) &= N_i^{k\mu}(\boldsymbol{y},z)u_{k,\mu}^{(0)}(\boldsymbol{x}) + M_i^{\mu}(\boldsymbol{y},z)\varphi_{,\mu}^{(0)}(\boldsymbol{x}) + w_i(\boldsymbol{x}) \\ \varphi^{(1)}(\boldsymbol{x},\boldsymbol{y},z) &= A^{k\mu}(\boldsymbol{y},z)u_{k,\mu}^{(0)}(\boldsymbol{x}) + \Xi^{\mu}(\boldsymbol{y},z)\varphi_{,\mu}^{(0)}(\boldsymbol{x}) + \gamma(\boldsymbol{x}), \end{aligned} \tag{4.6}$$

where w_i and γ are the homogeneous solutions. Equation (4.6) contains four unknown local functions of the microscopic variables, $N_i^{k\mu}$, M_i^{μ}, $A^{k\mu}$, Ξ^{μ}, which are determined via back-substitution of equation (4.6) into equations (4.5a) and (4.5b) to yield,

$$\begin{aligned} &\frac{1}{h_\mu}b_{i\mu|\mu}^{k\nu}(\boldsymbol{y},z) + b_{i3|3}^{k\nu}(\boldsymbol{y},z) = 0 && \frac{1}{h_\mu}b_{i\mu|\mu}^{\nu}(\boldsymbol{y},z) + b_{i3|3}^{\nu}(\boldsymbol{y},z) = 0 \\ &b_{ij}^{k\nu}(\boldsymbol{y},z)N_j^{\pm} = 0 \quad on\ Z^{\pm} && b_{ij}^{\nu}(\boldsymbol{y},z)N_j^{\pm} = 0 \quad on\ Z^{\pm} \\ &\frac{1}{h_\mu}\delta_{\mu|\mu}^{k\nu}(\boldsymbol{y},z) + \delta_{3|3}^{k\nu}(\boldsymbol{y},z) = 0 && \frac{1}{h_\mu}\delta_{\mu|\mu}^{\nu}(\boldsymbol{y},z) + \delta_{3|3}^{\nu}(\boldsymbol{y},z) = 0 \\ &\delta_i^{k\nu}(\boldsymbol{y},z)N_j^{\pm} = 0 \quad on\ Z^{\pm} && \delta_i^{\nu}(\boldsymbol{y},z)N_j^{\pm} = 0 \quad on\ Z^{\pm}, \end{aligned} \tag{4.7}$$

where the following definitions are made:

$$\begin{aligned} b_{ij}^{k\mu}(\boldsymbol{y},z) &= L_{ijm}N_m^{k\mu} + M_{ij}^{\mu}A^{k\mu} + c_{ijk\mu}, \quad b_{ij}^{\mu}(\boldsymbol{y},z) = L_{ijm}M_m^{\mu} + M_{ij}\Xi^{\mu} + e_{\mu ij} \\ \delta_i^{k\mu}(\boldsymbol{y},z) &= L_{im}^{*}N_m^{k\mu} - M_i^{*}A^{k\mu} + e_{ik\mu}, \quad \delta_i^{\mu}(\boldsymbol{y},z) = L_{im}^{*}M_m^{\mu} - M_i^{*}\Xi^{\mu} - \kappa_{i\mu}. \end{aligned} \tag{4.8}$$

The equations in (4.7) are solved entirely in the domain of the unit cell and are appropriately called unit cell problems. More unit cell problems will be derived in the process, as we will see in the sequel. We will refer to functions $b_{ij}^{k\mu}$, b_{ij}^{μ}, $\delta_i^{k\mu}$,δ_i^{μ} as the coefficient functions and from them, the effective coefficients may eventually be obtained.

In studies involving thin-walled structures, the possibility of finding an exact solution is important. In the case of the flexoelectric plate under examination, this solution involves the local functions $N_i^{3\lambda}$ and $A^{3\lambda}$ and is,

$$\begin{aligned} &N_1^{31} = -z, \quad N_2^{31} = N_3^{31} = 0 \\ &N_2^{32} = -z, \quad N_1^{32} = N_3^{32} = 0, \quad A^{31} = A^{32} = 0. \end{aligned} \tag{4.9}$$

This is readily shown by substituting equation (4.9) into the expressions for $b_{ij}^{k\mu}$ and $\delta_i^{k\mu}$ in equation (4.8) to first show that,

$$b_{ij}^{3\mu} = \delta_i^{3\mu} = 0. \tag{4.10}$$

and subsequently verifying that the first and third unit cell problems in equation (4.7) are satisfied.

Collectively, the main results stemming from the foregoing analysis may be summarized as follows:

$$\begin{aligned} &u_\mu^{(1)} = -zu_{3,\mu}^{(0)} + N_\mu^{\alpha\beta}u_{\alpha,\beta}^{(0)} + M_\mu^{\beta}\varphi_{,\beta}^{(0)} + w_\mu, \quad u_3^{(1)} = N_3^{\alpha\beta}u_{\alpha,\beta}^{(0)} + M_3^{\beta}\varphi_{,\beta}^{(0)} \\ &\varphi^{(1)} = A^{\alpha\beta}u_{\alpha,\beta}^{(0)} + \Xi^{\beta}\varphi_{,\beta}^{(0)} + \gamma, \quad \sigma_{ij}^{(0)} = b_{ij}^{\alpha\beta}u_{\alpha,\beta}^{(0)} + b_{ij}^{\beta}\varphi_{,\beta}^{(0)}, \quad D_i^{(0)} = \delta_i^{\alpha\beta}u_{\alpha,\beta}^{(0)} + \delta_i^{\beta}\varphi_{,\beta}^{(0)}. \end{aligned} \tag{4.11}$$

If we next apply the averaging process defined by equation (3.12) to $H_i^{(0)} = 0$ and $H^{*(0)} = 0$ from equations (4.2a) and (4.2b) and, in the resulting expressions, substitute the averaged stress and electric displacement, i.e., $\left\langle \sigma_{ij}^{(0)} \right\rangle$, and $\left\langle D_i^{(0)} \right\rangle$, we will get two equations for $u_\alpha^{(0)}$ and $\varphi^{(0)}$. Their solution, in

conjunction with the boundary conditions on the tangential surfaces, equation (3.2d), may be taken as $u_\alpha^{(0)} = \varphi^{(0)} = 0$. Consequently, equation (4.11) reduces to,

$$u_\mu^{(1)} = -zu_{3,\mu}^{(0)} + w_\mu, \quad u_3^{(1)} = w_3, \quad \varphi^{(1)} = \gamma, \quad \varepsilon_{ij}^{(0)} = \sigma_{ij}^{(0)} = E_i^{(0)} = D_i^{(0)} = 0. \tag{4.12}$$

To obtain the next order terms in the asymptotic expansions of mechanical displacement and electric potential, we turn our attention to the next set of balance equations coming from equations (4.2a) and (4.2b):

$$H_1^{(0)} = \left\langle H_1^{(0)} \right\rangle = 0 \quad \text{and} \quad H^{*(0)} = \left\langle H^{*(0)} \right\rangle = 0, \tag{4.13}$$

in which we substitute the expressions for $\sigma_{ij}^{(1)}$ and $D_i^{(1)}$ from equations (3.9c) and (3.10c) to get the following boundary value problems:

$$\begin{aligned} &L_{ik}^{(4)} u_k^{(2)} + M_i^{(4)} \varphi^{(2)} = -C_{i\mu\nu} w_{\mu,\nu} - P_{\nu i} \gamma_{,\nu} + \left[zC_{i\mu\nu} + c_{i3\mu\nu} \right] u_{3,\mu\nu}^{(0)} \\ &\left[L_{ijk} u_k^{(2)} + M_{ij}^{(2)(f)} \varphi^{(2)} + c_{ij\mu\nu} w_{\mu,\nu} + e_{vij} \gamma_{,\nu} - zc_{ij\mu\nu} u_{3,\mu\nu}^{(0)} \right] N_j^{\pm} = 0 \quad \text{on} \quad Z^{\pm}. \end{aligned} \tag{4.14a}$$

$$\begin{aligned} &\tau_k^{(4)} u_k^{(2)} + \tilde{\tau}^{(4)} \varphi^{(2)} = -G_{\mu\nu}^* w_{\mu,\nu} + I_\nu^* \gamma_{,\nu} + \left[zG_{\mu\nu}^* + \tilde{\mu}_{\mu\nu 3}^{(3)} \right] u_{3,\mu\nu}^{(0)} \\ &\left[L_{ik}^{*(2)} u_k^{(2)} - M_i^* \varphi^{(2)} + e_{i\mu\nu} w_{\mu,\nu} - \kappa_{i\nu} \gamma_{,\nu} - \left(ze_{i\mu\nu} + \mu_{i\mu\nu 3}^{(f)} \right) u_{3,\mu\nu}^{(0)} \right] N_j^{\pm} = 0 \quad \text{on} \quad Z^{\pm}. \end{aligned} \tag{4.14b}$$

The definitions of the differential operators and variables appearing in equations (4.14a) and (4.14b) are given in Appendix A. The separation of variables on the RHS of equations (4.14a) and (4.14b) prompts a solution in the form of,

$$\begin{aligned} u_i^{(2)} &= N_i^{(1)\mu\nu}(\boldsymbol{y}, z) w_{\mu,\nu}(\boldsymbol{x}) + M_i^{(1)\nu}(\boldsymbol{y}, z) \gamma_{,\nu}(\boldsymbol{x}) - N_i^{*(2)\mu\nu}(\boldsymbol{y}, z) u_{3,\mu\nu}^{(0)}(\boldsymbol{x}) + w_i^{(2)}(\boldsymbol{x}) \\ \varphi^{(2)} &= A^{(1)\mu\nu}(\boldsymbol{y}, z) w_{\mu,\nu}(\boldsymbol{x}) + \Xi^{(1)\nu}(\boldsymbol{y}, z) \gamma_{,\nu}(\boldsymbol{x}) - A^{*(2)\mu\nu}(\boldsymbol{y}, z) u_{3,\mu\nu}^{(0)}(\boldsymbol{x}) + \gamma^{(2)}(\boldsymbol{x}). \end{aligned} \tag{4.15a}$$

where, again, $w_i^{(2)}$ and $\gamma^{(2)}$ are homogeneous solutions. Back substitution of equation (4.15a) into equations (4.14a) and (4.14b), gives, after comparing like terms, the following six unit cell problems for the determination of as many local functions, $N_i^{(1)\mu\nu}$, $A^{(1)\mu\nu}$, and so on appearing in equation (4.15a),

$$\begin{aligned} &\frac{1}{h_\gamma} b_{i\gamma|\gamma}^{(1)m\nu}(\boldsymbol{y}, z) + b_{i3|3}^{(1)m\nu}(\boldsymbol{y}, z) = 0 && \frac{1}{h_\gamma} b_{i\gamma|\gamma}^{(1)\nu}(\boldsymbol{y}, z) + b_{i3|3}^{(1)\nu}(\boldsymbol{y}, z) = 0 \\ &b_{ij}^{(1)m\nu}(\boldsymbol{y}, z) N_j^{\pm} = 0 \quad \textit{on } Z^{\pm} && b_{ij}^{(1)\nu}(\boldsymbol{y}, z) N_j^{\pm} = 0 \quad \textit{on } Z^{\pm} \\ &\frac{1}{h_\gamma} \delta_{\gamma|\gamma}^{(1)m\nu}(\boldsymbol{y}, z) + \delta_{3|3}^{(1)m\nu}(\boldsymbol{y}, z) = 0 && \frac{1}{h_\gamma} \delta_{\gamma|\gamma}^{(1)\nu}(\boldsymbol{y}, z) + \delta_{3|3}^{(1)\nu}(\boldsymbol{y}, z) = 0 \\ &\delta_i^{(1)m\nu}(\boldsymbol{y}, z) N_i^{\pm} = 0 \quad \textit{on } Z^{\pm} && \delta_i^{(1)\nu}(\boldsymbol{y}, z) N_i^{\pm} = 0 \quad \textit{on } Z^{\pm} \\ &\frac{1}{h_\gamma} B_{i\gamma|\gamma}^{*\mu\nu}(\boldsymbol{y}, z) + B_{i3|3}^{*\mu\nu}(\boldsymbol{y}, z) = 0 && \frac{1}{h_\gamma} \Delta_{\gamma|\gamma}^{*(f)\mu\nu}(\boldsymbol{y}, z) + \Delta_{3|3}^{*(f)\mu\nu}(\boldsymbol{y}, z) = 0 \\ &B_{ij}^{*\mu\nu}(\boldsymbol{y}, z) N_j^{\pm} = 0 \quad \textit{on } Z^{\pm} && \Delta_i^{*(f)\mu\nu}(\boldsymbol{y}, z) N_i^{\pm} = 0 \quad \textit{on } Z^{\pm}, \end{aligned} \tag{4.15b}$$

where the following definitions are made:

$$\begin{aligned} &b_{ij}^{(1)m\nu} = L_{ijm} N_m^{(1)m\nu} + M_{ij}^{(2)(f)} A^{(1)m\nu} + c_{ijm\nu}, \quad b_{ij}^{(1)\nu} = L_{ijm} M_m^{(1)\nu} + M_{ij}^{(2)(f)} \Xi^{(1)\nu} + e_{\nu ij} \\ &\delta_i^{(1)m\nu} = L_{im}^{*(2)} N_m^{(1)m\nu} - M_i^* A^{(1)m\nu} + e_{im\nu}, \quad \Delta_i^{*(f)\mu\nu} = L_{im}^{*(2)} N_m^{*(2)\mu\nu} - M_i^* A^{*(2)\mu\nu} + \left[ze_{i\mu\nu} + \mu_{i\mu\nu 3}^{(f)} \right] \\ &B_{ij}^{*\mu\nu} = L_{ijm} N_m^{*(2)\mu\nu} + M_{ij}^{(2)(f)} A^{*(2)\mu\nu} + zc_{ij\mu\nu}, \quad \delta_i^{(1)\nu} = L_{im}^{*(2)} M_m^{(1)\nu} - \Xi^{(1)\nu} - \kappa_{i\nu}. \end{aligned} \tag{4.16}$$

These coefficient functions are related to first-gradient homogenization and from them, the effective in-plane and out-of-plane elastic (extensional, bending, coupling), piezoelectric and dielectric coefficients will be determined. Differential operators appearing in equation (4.16) are defined in Appendix A. Notice from equations (4.8), (4.16), (A.1), and (A.2) that the flexoelectric coefficients have negligible influence on the elastic and piezoelectric coefficient functions so that $b_{ij}^{(1)3\nu} \approx b_{ij}^{3\nu} = 0$ and $\delta_i^{(1)3\nu} \approx \delta_i^{3\nu} = 0$. Thus, we can let superscript $m \to \mu$ in the first and third expressions in equation (4.15b) and, as a result, the macroscopic constant w_3 may be set equal to zero as in the first-gradient elasticity model in Kalamkarov [49]. In view of this as well as equation (4.12), the leading terms in the asymptotic expansions of stress and electric displacement are given by:

$$\sigma_{ij}^{(1)} = b_{ij}^{(1)\mu\nu} w_{\mu,\nu} + b_{ij}^{(1)\nu} \gamma_{,\nu} + B_{ij}^{*\mu\nu} u_{3,\mu\nu}^{(0)} \quad D_i^{(1)} = \delta_i^{(1)\mu\nu} w_{\mu,\nu} + \delta_i^{(1)\nu} \gamma_{,\nu} + \Delta_i^{*(f)\mu\nu} u_{3,\mu\nu}^{(0)}. \tag{4.17}$$

5. Second-gradient homogenization

We begin our analysis by substituting equation (4.15a) into equations (3.9a)–(3.10c) for $n = 1$ or $n = 2$ and, after ignoring third-order gradient of $u_3^{(0)}$, we obtain the following expressions for strain, strain gradient, electric field, field gradient, mechanical stress, and electric displacement:

$$\begin{aligned}
\varepsilon_{\alpha\beta}^{(2)} &= A_{\alpha\beta}^{\mu\nu\lambda} w_{\mu,\nu\lambda} + \Gamma_{\alpha\beta}^{\nu\lambda} \gamma_{,\nu\lambda} + \frac{1}{2}\left(w_{\alpha,\beta}^{(2)} + w_{\beta,\alpha}^{(2)}\right) + \frac{1}{2}\left(\frac{1}{h_\beta} u_{\alpha|\beta}^{(3)} + \frac{1}{h_\alpha} u_{\beta|\alpha}^{(3)}\right) \\
\varepsilon_{3\beta}^{(2)} &= \frac{1}{2} A_{3\beta}^{\mu\nu\lambda} w_{\mu,\nu\lambda} + \frac{1}{2} \Gamma_{3\beta}^{\nu\lambda} \gamma_{,\nu\lambda} + \frac{1}{2}\left(\frac{1}{h_\beta} u_{3|\beta}^{(3)} + u_{\beta|3}^{(3)}\right), \quad \varepsilon_{33}^{(2)} = u_{3|3}^{(3)}.
\end{aligned} \tag{5.1a}$$

$$\begin{aligned}
\omega_{\alpha\beta\gamma}^{(1)} &= \Delta_{\alpha\beta\gamma}^{\mu\nu\lambda} w_{\mu,\nu\lambda} + E_{\alpha\beta\gamma}^{\nu\lambda} \gamma_{,\nu\lambda} + \frac{1}{2}\frac{1}{h_\gamma}\frac{\partial}{\partial y_\gamma}\left(\frac{1}{h_\beta} u_{\alpha|\beta}^{(3)} + \frac{1}{h_\alpha} u_{\beta|\alpha}^{(3)}\right) \\
\omega_{3\beta\gamma}^{(1)} &= \frac{1}{2} \Delta_{3\beta\gamma}^{\mu\nu\lambda} w_{\mu,\nu\lambda} + \frac{1}{2} E_{3\beta\gamma}^{\nu\lambda} \gamma_{,\nu\lambda} + \frac{1}{2}\frac{1}{h_\gamma}\frac{\partial}{\partial y_\gamma}\left(\frac{1}{h_\beta} u_{3|\beta}^{(3)} + u_{\beta|3}^{(3)}\right) \\
\omega_{33\gamma}^{(1)} &= \Delta_{33\gamma}^{\mu\nu\lambda} w_{\mu,\nu\lambda} + E_{33\gamma}^{\nu\lambda} \gamma_{,\nu\lambda} + \frac{1}{h_\gamma}\frac{\partial}{\partial y_\gamma}\left(u_{3|3}^{(3)}\right) \\
\omega_{\alpha\beta3}^{(1)} &= \Delta_{\alpha\beta3}^{\mu\nu\lambda} w_{\mu,\nu\lambda} + E_{\alpha\beta3}^{\nu\lambda} \gamma_{,\nu\lambda} + \frac{1}{2}\frac{\partial}{\partial z}\left(\frac{1}{h_\beta} u_{\alpha|\beta}^{(3)} + \frac{1}{h_\alpha} u_{\beta|\alpha}^{(3)}\right) \\
\omega_{3\beta3}^{(1)} &= \frac{1}{2} \Delta_{3\beta3}^{\mu\nu\lambda} w_{\mu,\nu\lambda} + \frac{1}{2} E_{3\beta3}^{\nu\lambda} \gamma_{,\nu\lambda} + \frac{1}{2}\frac{\partial}{\partial z}\left(\frac{1}{h_\beta} u_{3|\beta}^{(3)} + u_{\beta|3}^{(3)}\right), \quad \omega_{333}^{(1)} = u_{3|33}^{(3)}.
\end{aligned} \tag{5.1b}$$

$$E_\beta^{(2)} = I_\beta^{\mu\nu\lambda} w_{\mu,\nu\lambda} + J_\beta^{\nu\lambda} \gamma_{,\nu\lambda} - \gamma_{,\beta}^{(2)} - \frac{1}{2}\frac{1}{h_\beta} \varphi_{|\beta}^{(3)}, \quad E_3^{(2)} = -\varphi_{|3}^{(3)}. \tag{5.1c}$$

$$\begin{aligned}
V_{\alpha\beta}^{(1)} &= H_{\alpha\beta}^{\mu\nu\lambda} w_{\mu,\nu\lambda} + Z_{\alpha\beta}^{\nu\lambda} \gamma_{,\nu\lambda} - \frac{1}{h_\alpha h_\beta} \varphi_{|\alpha\beta}^{(3)} \\
V_{3\beta}^{(1)} &= H_{3\beta}^{\mu\nu\lambda} w_{\mu,\nu\lambda} + Z_{3\beta}^{\nu\lambda} \gamma_{,\nu\lambda} - \frac{1}{h_\beta}\frac{\partial}{\partial y_\beta} \varphi_{|3}^{(3)}, \quad V_{33}^{(1)} = -\varphi_{|33}^{(3)}.
\end{aligned} \tag{5.1d}$$

$$\begin{aligned}
\sigma_{ij}^{(2)} &= \tilde{b}_{ij}^{\mu\nu\lambda} w_{\mu,\nu\lambda} + \tilde{b}_{ij}^{\nu\lambda} \gamma_{,\nu\lambda} + c_{ij\mu\beta} w_{\mu,\beta}^{(2)} + e_{\beta ij} \gamma_{,\beta}^{(2)} + L_{ijk} u_k^{(3)} + M_{ij}^{(2)(f)} \varphi^{(3)} \\
D_i^{(2)} &= \tilde{\delta}_i^{\mu\nu\lambda} w_{\mu,\nu\lambda} + \tilde{\delta}_i^{(2)\nu\lambda} \gamma_{,\nu\lambda} + e_{i\mu\beta} w_{\mu,\beta}^{(2)} - \kappa_{i\beta} \gamma_{,\beta}^{(2)} + L_{ik}^{*(2)} u_k^{(3)} - M_i^* \varphi^{(3)}.
\end{aligned} \tag{5.1e}$$

The different microscopic variables and differential operators appearing in equations (5.1a)–(5.1e) are defined in Appendix A. In contrast to the expressions in equation (4.17), the variables in equations (5.1a)–(5.1e) are functions of the second gradient of the macroscopic variables of displacement, w_μ, and electric potential, γ.

Equation (4.1a) gives the next set of problems that must be solved, namely,

$$H_i^{(1)} = \left\langle H_i^{(1)} \right\rangle, \quad H^{*(1)} = \left\langle H^{*(1)} \right\rangle, \tag{5.2}$$

which, on account of equations (4.1b), (4.2a), (4.2b) and the averaging result in equation (3.12), and upon ignoring third-gradient terms, results in the following boundary value problems:

$$\begin{aligned} &\sigma_{i\beta.\beta}^{(1)} + \frac{1}{h_\beta}\sigma_{i\beta|\beta}^{(2)} + \sigma_{i3|3}^{(2)} = \left\langle \sigma_{i\beta}^{(1)} \right\rangle_{,\beta} && D_{\beta,\beta}^{(1)} + \frac{1}{h_\beta} D_{\beta|\beta}^{(2)} + D_{3|3}^{(2)} = \left\langle D_\beta^{(1)} \right\rangle_{,\beta} . \\ &\sigma_{ij}^{(2)} N_j^{\pm} = 0 \quad \text{on } Z^{\pm} && D_i^{(2)} N_i^{\pm} = 0 \quad \text{on } Z^{\pm} \end{aligned} \tag{5.3}$$

Substituting equations (5.1a)–(5.1e) into equation (5.3) results in the following system which is essentially the complement of equations (4.14a) and (4.14b):

$$\begin{aligned} L_{ik}^{(4)} u_k^{(3)} + M_i^{(4)} \varphi^{(3)} =& -\left(b_{i\lambda}^{(1)\mu\nu} - \left\langle b_{i\lambda}^{(1)\mu\nu} \right\rangle + \tilde{b}_i^{(3)\mu\nu\lambda} \right) w_{\mu,\nu\lambda} - \left(b_{i\lambda}^{(1)\nu} - \left\langle b_{i\lambda}^{(1)\nu} \right\rangle + \tilde{b}_i^{(3)\nu\lambda} \right) \gamma_{,\nu\lambda} + \\ & - C_{i\mu\lambda} w_{\mu,\lambda}^{(2)} - P_{\lambda i} \gamma_{,\lambda}^{(2)} \\ & \left[L_{ijk} u_k^{(3)} + M_{ij}^{(2)(f)} \varphi^{(3)} + \tilde{b}_{ij}^{\mu\nu\lambda} w_{\mu,\nu\lambda} + \tilde{b}_{ij}^{\nu\lambda} \gamma_{,\nu\lambda} + c_{ij\mu\lambda} w_{\mu,\lambda}^{(2)} + e_{\lambda ij} \gamma_{,\lambda}^{(2)} \right] N_j^{\pm} = 0 \quad \text{on } Z^{\pm}. \end{aligned} \tag{5.4a}$$

$$\begin{aligned} \tilde{\tau}_k^{(4)} u_k^{(3)} - \tilde{\tau}^{(4)} \varphi^{(3)} =& -\left(\delta_\lambda^{(1)\mu\nu} - \left\langle \delta_\lambda^{(1)\mu\nu} \right\rangle + \tilde{\sigma}^{(3)\mu\nu\lambda} \right) w_{\mu,\nu\lambda} - \left(\delta_\lambda^{(1)\nu} - \left\langle \delta_\lambda^{(1)\nu} \right\rangle + \tilde{\sigma}^{*(3)\nu\lambda} \right) \gamma_{,\nu\lambda} + \\ & - G_{\mu\nu}^{*} w_{\mu,\nu}^{(2)} + I_\nu^{*} \gamma_{,\nu}^{(2)} \\ & \left[L_{ik}^{*(2)} u_k^{(3)} - M_i^{*} \varphi^{(3)} + \tilde{\delta}_i^{\mu\nu\lambda} w_{\mu,\nu\lambda} + \tilde{\delta}_i^{(2)\nu\lambda} \gamma_{,\nu\lambda} + e_{i\mu\nu} w_{\mu,\nu}^{(2)} - \kappa_{i\nu} \gamma_{,\nu}^{(2)} \right] N_\iota^{\pm} = 0 \quad \text{on } Z^{\pm}. \end{aligned} \tag{5.4b}$$

Variables and differential operators appearing in equations (5.4a) and (5.4b) are defined in Appendix A. As in the case of equations (4.14a) and (4.14b), we can write down the solution of $u_k^{(3)}$ and $\varphi^{(3)}$ in the form of,

$$\begin{aligned} u_i^{(3)} &= N_i^{(2)\mu\nu\lambda}(\boldsymbol{y}, z) w_{\mu,\nu\lambda}(\boldsymbol{x}) + M_i^{(2)\nu\lambda}(\boldsymbol{y}, z) \gamma_{,\nu\lambda}(\boldsymbol{x}) + N_i^{(1)\nu\lambda} w_{\nu,\lambda}^{(2)} + M_i^{(1)\nu} \gamma_{,\nu}^{(2)} + w_i^{(3)}(\boldsymbol{x}) \\ \varphi^{(3)} &= A^{(2)\mu\nu\lambda}(\boldsymbol{y}, z) u_{\mu,\nu\lambda}^{(0)}(\boldsymbol{x}) + \Xi^{(2)\nu\lambda}(\boldsymbol{y}, z) \varphi_{,\nu\lambda}^{(0)}(\boldsymbol{x}) + A^{(1)\nu\lambda} w_{\nu,\lambda}^{(2)} + \Xi^{\nu} \gamma_{,\nu}^{(2)} + \gamma^{(3)}(\boldsymbol{x}). \end{aligned} \tag{5.5}$$

To calculate the local functions appearing in equation (5.5), we back-substitute it into equations (5.4a) and (5.4b) to obtain eight unit cell problems to accompany the set of six appearing in equation (4.15b). Four of these are identical to the first four expressions in equation (4.15b) while the remaining four, necessary for the determination of local functions, $N_i^{(2)\mu\nu\lambda}$, $M_i^{(2)\nu\lambda}$, $A^{(2)\mu\nu\lambda}$, $\Xi^{(2)\nu\lambda}$, are given in equation (5.6). As is evident, this second set of problems stemming from second-gradient asymptotic homogenization is related to the second gradient of the mechanical strain and the electric potential. Their solution yields the coefficient functions which, when averaged over the volume of the unit cell will produce the corresponding effective coefficients characterizing the homogenized flexoelectric plate. We also note that the local functions, much like their counterparts in equation (4.15a), are dependent on only the microscopic variables and exhibit periodicity in the y_1 and y_2 directions.

$$\begin{aligned} &b_{i\lambda}^{(1)\mu\nu} - \left\langle b_{i\lambda}^{(1)\mu\nu} \right\rangle + \frac{1}{h_\gamma} B_{i\gamma|\gamma}^{\mu\nu\lambda} + B_{i3|3}^{\mu\nu\lambda} = 0 && b_{i\lambda}^{(1)\nu} - \left\langle b_{i\lambda}^{(1)\nu} \right\rangle + \frac{1}{h_\gamma} B_{i\gamma|\gamma}^{\nu\lambda} + B_{i3|3}^{\nu\lambda} = 0 \\ &B_{ij}^{\mu\nu\lambda} N_j^{\pm} = 0 \quad \text{on } Z^{\pm} && B_{ij}^{\nu\lambda} N_j^{\pm} = 0 \quad \text{on } Z^{\pm} \\ &\delta_\lambda^{(1)\mu\nu} - \left\langle \delta_\lambda^{(1)\mu\nu} \right\rangle + \frac{1}{h_\gamma} \Delta_{\gamma|\gamma}^{\mu\nu\lambda} + \Delta_{3|3}^{\mu\nu\lambda} = 0 && \delta_\lambda^{(1)\nu} - \left\langle \delta_\lambda^{(1)\nu} \right\rangle + \frac{1}{h_\gamma} \Delta_{\gamma|\gamma}^{(f)\nu\lambda} + \Delta_{3|3}^{(f)\nu\lambda} = 0 \\ &\Delta_i^{\mu\nu\lambda} N_i^{\pm} = 0 \quad \text{on } Z^{\pm} && \Delta_i^{(f)\nu\lambda} N_i^{\pm} = 0 \quad \text{on } Z^{\pm} \end{aligned} . \tag{5.6}$$

Here, we make the following definitions for the various coefficient functions:

$$\begin{aligned} B_{ij}^{\mu\nu\lambda} &= L_{ijk}N_k^{(2)\mu\nu\lambda} + M_{ij}^{(2)(f)}A^{(2)\mu\nu\lambda} + \tilde{b}_{ij}^{\mu\nu\lambda}, \quad B_{ij}^{\nu\lambda} = L_{ijk}M_k^{(2)\nu\lambda} + M_{ij}^{(2)(f)}\Xi^{(2)\nu\lambda} + \tilde{b}_{ij}^{\nu\lambda} \\ \Delta_i^{\mu\nu\lambda} &= L_{ik}^{*(2)}N_k^{(2)\mu\nu\lambda} - M_i^{*}A^{(2)\mu\nu\lambda} + \tilde{\delta}_i^{\mu\nu\lambda}, \quad \Delta_i^{(f)\nu\lambda} = L_{ik}^{*(2)}M_k^{(2)\nu\lambda} - M_i^{*}\Xi^{(2)\nu\lambda} + \tilde{\delta}_i^{(2)\nu\lambda}. \end{aligned} \tag{5.7a}$$

In terms of the coefficient functions of equation (5.7a), the mechanical stress and electric displacement terms are given by,

$$\begin{aligned} \sigma_{ij}^{(2)} &= B_{ij}^{\mu\nu\lambda}w_{\mu,\nu\lambda} + B_{ij}^{\nu\lambda}\gamma_{,\nu\lambda} + b_{ij}^{(1)\nu\lambda}w_{\mu,\lambda}^{(2)} + b_{ij}^{(1)\nu}\gamma_{,\nu}^{(2)} \\ D_i^{(2)} &= \Delta_i^{\mu\nu\lambda}w_{\mu,\nu\lambda} + \Delta_i^{(f)\nu\lambda}\gamma_{,\nu\lambda} + \delta_i^{(1)\nu\lambda}w_{\mu,\lambda}^{(2)} + \delta_i^{(1)\nu}\gamma_{,\nu}^{(2)}. \end{aligned} \tag{5.7b}$$

An important point to be made is that in the preceding analysis, we assumed that the material coefficients, $c_{ijkl}(\boldsymbol{y},z)$, $e_{ijk}(\boldsymbol{y},z)$, $\mu_{ijkl}(\boldsymbol{y},z)$, and so on are smooth. However, we may generalize the unit cell problems to include piecewise-smooth coefficients with discontinuities at contact surfaces between different constituents by imposing the appropriate continuity conditions, see Kalamkarov [49]. Thus,

$$\begin{aligned} &\left[\!\left[N_m^{(1)\mu\nu}\right]\!\right] = 0 \quad \left(N_m^{(1)\mu\nu} \leftrightarrow M_m^{(1)\nu} \leftrightarrow A^{(1)\mu\nu} \leftrightarrow \Xi^{(1)\mu} \leftrightarrow N_m^{(2)\mu\nu\lambda} \leftrightarrow M_m^{(2)\nu\lambda}\ldots\right) \\ &\left[\!\left[\frac{1}{h_\gamma}n_\gamma^{(k)}b_{i\gamma}^{(1)\mu\nu} + n_3^{(k)}b_{i3}^{(1)\mu\nu}\right]\!\right] = 0 \quad \left(b_{ij}^{(1)\mu\nu} \leftrightarrow b_{ij}^{(1)\nu} \leftrightarrow \delta_i^{(1)\mu\nu} \leftrightarrow \delta_i^{(1)\nu} \leftrightarrow B_{ij}^{\mu\nu\lambda} \leftrightarrow B_{ij}^{\nu\lambda}\ldots\right) \end{aligned} \tag{5.8}$$

where $[\![...]\!]$ denotes a jump in a function at a contact surface and $n_i^{(k)}$ is the unit normal vector at this surface as related to the (y_1, y_2, z) coordinate system. Before closing, let us set $w_3^{(2)} = 0$, like its counterpart w_3, and let us make the following definitions,

$$\begin{aligned} &\delta w_\mu + \delta^2 w_\mu^{(2)} + \delta^3 w_\mu^{(3)} + \cdots = \mathrm{v}_\mu + O(\delta^2), \quad \delta\gamma + \delta^2\gamma^{(2)} + \delta^3\gamma^{(3)} + \cdots = \varphi^* + O(\delta^2) \\ &\delta w_{\mu,\nu} + \delta^2 w_{\mu,\nu}^{(2)} + \cdots = \mathrm{v}_{\mu,\nu} + O(\delta^2) = \varepsilon_{\mu\nu}^{(M)} + O(\delta^2), \quad u_3^{(0)} = w, \quad -u_{3,\nu\lambda}^{(0)} = \tau_{\mu\nu}^{(M)} \\ &\delta\gamma_{,\nu} + \delta^2\gamma_{,\nu}^{(2)} + \cdots = \varphi_{,\nu}^* + O(\delta^2) = E_\nu^{(M)} + O(\delta^2) \\ &\delta\gamma_{,\nu\lambda}^{(2)} + \cdots = V_{\nu\lambda}^{(M)} + O(\delta^2) = E_{\nu,\lambda}^{(M)} + O(\delta^2) \\ &\delta w_{\mu,\nu\lambda}^{(2)} + \cdots = \varepsilon_{\mu\nu,\lambda}^{(M)} + O(\delta^2) = \omega_{\mu\nu\lambda}^{(M)} + O(\delta^2), \end{aligned} \tag{5.9}$$

for the macroscopic tangential displacement, v_μ, macroscopic strain, $\varepsilon_{\mu\nu}^{(M)}$, and strain gradient, $\omega_{\mu\nu\lambda}^{(M)}$, macroscopic potential, φ^*, electric field, $E_\nu^{(M)}$, and field gradient, $V_{\nu\lambda}^{(M)}$ as well as the transverse displacement, w, and let us combine the results in equations (3.11), (4.12), (4.15a), (4.17), (5.5), and (5.7b) to obtain the asymptotic approximations of mechanical displacement, electric potential, mechanical stress, and electric displacement as given in equations (5.10) and (5.11). In the next section, we will compare these results with other published works and elucidate the meaning of the different variables.

$$\begin{aligned} u_\alpha &= (\mathrm{v}_1 - \gamma w_{,\alpha}) + \delta\left(N_\alpha^{(1)\mu\nu}\varepsilon_{\mu\nu}^{(M)} + M_\alpha^{(1)\nu}E_\nu^{(M)}\right) + \\ &\quad + \delta^2\left(N_\alpha^{*(2)\mu\nu}\tau_{\mu\nu}^{(M)} + N_\alpha^{(2)\mu\nu\lambda}\omega_{\mu\nu\lambda}^{(M)} + M_i^{(2)\nu\lambda}V_{\nu\lambda}^{(M)}\right) \\ u_3 &= w + \delta\left(N_\alpha^{(1)\mu\nu}\varepsilon_{\mu\nu}^{(M)} + M_3^{(1)\nu}E_\nu^{(M)}\right) + \delta^2\left(N_3^{*(2)\mu\nu}\tau_{\mu\nu}^{(M)} + N_3^{(2)\mu\nu\lambda}\omega_{\mu\nu\lambda}^{(M)} + M_3^{(2)\nu\lambda}V_{\nu\lambda}^{(M)}\right) \\ \varphi &= \varphi^* + \delta\left(A^{(1)\mu\nu}\varepsilon_{\mu\nu}^{(M)} + \Xi^{(1)\nu}E_\nu^{(M)}\right) + \delta^2\left(A^{*(2)\nu\lambda}\tau_{\mu\nu}^{(M)} + A^{(2)\mu\nu\lambda}\omega_{\mu\nu\lambda}^{(M)} + \Xi^{(2)\nu\lambda}V_{\nu\lambda}^{(M)}\right). \end{aligned} \tag{5.10}$$

$$\begin{aligned} \sigma_{ij} &= b_{ij}^{(1)\mu\nu}\varepsilon_{\mu\nu}^{(M)} + b_{ij}^{(1)\nu}E_\nu^{(M)} + \delta\left(B_{ij}^{*\nu\lambda}\tau_{\nu\lambda}^{(M)} + B_{ij}^{\mu\nu\lambda}\omega_{\mu\nu\lambda}^{(M)} + B_{ij}^{\nu\lambda}V_{\nu\lambda}^{(M)}\right) \\ D_i &= \delta_i^{(1)\mu\nu}\varepsilon_{\mu\nu}^{(M)} + \delta_i^{(1)\nu}E_\nu^{(M)} + \delta\left(\Delta_i^{*(f)\nu\lambda}\tau_{\nu\lambda}^{(M)} + \Delta_i^{\mu\nu\lambda}\omega_{\mu\nu\lambda}^{(M)} + \Delta_i^{(f)\nu\lambda}V_{\nu\lambda}^{(M)}\right). \end{aligned} \tag{5.11}$$

6. Governing equations, macroscopic problem, and effective coefficients

In the analysis of thin-walled plate and shell structures, it is sometimes useful to deal with the force and moment resultants, $N_{ij}^{(f)}$ and $M_{ij}^{(f)}$, respectively. In the language of the current model, these are defined as,

$$N_{\alpha\beta}^{(f)} = \delta\langle\sigma_{\alpha\beta}\rangle, \quad M_{\alpha\beta}^{(f)} = \delta^2\langle z\sigma_{\alpha\beta}\rangle. \tag{6.1}$$

Applying the averaging operation defined by equation (3.12) to equation (5.11), gives, on account of equation (6.1), the following expressions for the force and moment resultants as well as the averaged stresses and electric displacement:

$$\begin{aligned}
\langle\sigma_{ij}\rangle &= \left\langle b_{ij}^{(1)\mu\nu}\right\rangle\varepsilon_{\mu\nu}^{(M)} + \left\langle b_{ij}^{(1)\nu}\right\rangle E_{\nu}^{(M)} + \delta\left(\left\langle B_{ij}^{*\nu\lambda}\right\rangle\tau_{\nu\lambda}^{(M)} + \left\langle B_{ij}^{\mu\nu\lambda}\right\rangle\omega_{\mu\nu\lambda}^{(M)} + \left\langle B_{ij}^{\nu\lambda}\right\rangle V_{\nu\lambda}^{(M)}\right)\\
N_{\alpha\beta}^{(f)} &= \delta\left(\left\langle b_{\alpha\beta}^{(1)\mu\nu}\right\rangle\varepsilon_{\mu\nu}^{(M)} + \left\langle b_{\alpha\beta}^{(1)\nu}\right\rangle E_{\nu}^{(M)}\right) + \delta^2\left(\left\langle B_{\alpha\beta}^{*\nu\lambda}\right\rangle\tau_{\nu\lambda}^{(M)} + \left\langle B_{\alpha\beta}^{\mu\nu\lambda}\right\rangle\omega_{\mu\nu\lambda}^{(M)} + \left\langle B_{\alpha\beta}^{\nu\lambda}\right\rangle V_{\nu\lambda}^{(M)}\right)\\
M_{\alpha\beta}^{(f)} &= \delta^2\left(\left\langle zb_{\alpha\beta}^{(1)\mu\nu}\right\rangle\varepsilon_{\mu\nu}^{(M)} + \left\langle zb_{\alpha\beta}^{(1)\nu}\right\rangle E_{\nu}^{(M)}\right) + \delta^3\left(\left\langle zB_{\alpha\beta}^{*\nu\lambda}\right\rangle\tau_{\nu\lambda}^{(M)} + \left\langle zB_{\alpha\beta}^{\mu\nu\lambda}\right\rangle\omega_{\mu\nu\lambda}^{(M)} +\right.\\
&\quad \left. + \left\langle zB_{\alpha\beta}^{\nu\lambda}\right\rangle V_{\nu\lambda}^{(M)}\right)\\
\delta\langle D_{\alpha}\rangle &= \delta\left(\left\langle\delta_{\alpha}^{(1)\mu\nu}\right\rangle\varepsilon_{\mu\nu}^{(M)} + \left\langle\delta_{\alpha}^{(1)\nu}\right\rangle E_{\nu}^{(M)}\right) + \delta^2\left(\left\langle\Delta_{\alpha}^{*(f)\nu\lambda}\right\rangle\tau_{\nu\lambda}^{(M)} + \langle\Delta_{\alpha}^{\mu\nu\lambda}\rangle\omega_{\mu\nu\lambda}^{(M)} +\right.\\
&\quad \left. + \left\langle\Delta_{\alpha}^{(f)\nu\lambda}\right\rangle V_{\nu\lambda}^{(M)}\right).
\end{aligned} \tag{6.2}$$

Examination of equations (5.10) and (6.2) reveals that $\varepsilon_{\mu\nu}^{(M)}$ are the mid-surface strains, $\tau_{11}^{(M)}$ and $\tau_{22}^{(M)}$ are the bending curvatures of the mid-surface in the x_1–x_3 and x_2–x_3 planes, respectively, while $2\tau_{12}^{(M)}$ is the twisting curvature associated with torsion of the middle surface, see Hadjiloizi et al. [51,53]. Furthermore, $\delta\left\langle b_{\alpha\beta}^{(1)\mu\nu}\right\rangle$ and $\delta^3\left\langle zB_{\alpha\beta}^{*\nu\lambda}\right\rangle$ are the effective extensional and effective bending elastic coefficients, while $\delta^2\left\langle B_{\alpha\beta}^{*\nu\lambda}\right\rangle$, $\delta^2\left\langle zb_{\alpha\beta}^{(1)\mu\nu}\right\rangle$ are the effective coupling elastic coefficients, see Kalamkarov [49] and Hadjiloizi et al. [51,53]. Next, $\delta\left\langle b_{\alpha\beta}^{(1)\nu}\right\rangle$, $\delta\left\langle\delta_{i}^{(1)\mu\nu}\right\rangle$ are the effective in-plane piezoelectric coefficients, $\delta^2\left\langle\Delta_{ij}^{*(f)\nu\lambda}\right\rangle$ are their out-of-plane counterparts while $-\delta\langle\delta_{i}^{\nu}\rangle$ are the effective dielectric permittivity coefficients. In addition, $\delta^2\left\langle B_{\alpha\beta}^{\mu\nu\lambda}\right\rangle$ and $\delta^3\left\langle zB_{ij}^{\mu\nu\lambda}\right\rangle$ are effective coefficients coupling, respectively, force and moment resultants with strain gradient and, correspondingly, $-\delta^2\left\langle\Delta_{i}^{(f)\nu\lambda}\right\rangle$ are the effective coefficients coupling electric displacement to field gradient. It should be noted that this latter set of effective coefficients arises in the homogenized flexoelectric reinforced plate even though we originally ignored this particular behavior by the *individual* constituents. In other words, these effective coefficients show up in the homogenized structure even though material tensors r_{ijklm} and h_{ijk}, see equation (2.3), were neglected from the eventual formulation of the problem as it appears in equation (3.2d). Equation (6.2) further reveals that $-\delta^2\left\langle B_{\alpha\beta}^{\nu\lambda}\right\rangle$, $\delta^2\left\langle\Delta_{ij}^{(f)\nu\lambda}\right\rangle$ are the effective in-plane flexoelectric coefficients while $\delta^3\left\langle zB_{ij}^{\nu\lambda}\right\rangle$ are their out-of-plane counterparts coupling moment resultants with electric field gradients.

Comparing the foregoing results with other published works, we would like to point out the following observations. First, if we ignore any strain-gradient and field-gradient effects, then the expressions in equations (5.10), (5.11), and (6.2) converge to previously established results such as those in Hadjiloizi et al. [51–54]. If we further limit our analysis to strictly elastic behavior and first-gradient homogenization and also ignore any corrugations of the top and bottom surfaces, these results converge to the familiar classical plate model, see Gibson [73] and Reddy [74]. Second, because we follow a fully coupled approach, the effective elastic (for example) coefficients are functions of not only the elastic parameters of the individual constituents but also of the piezoelectric ones, see, for example, equation (4.16). This

will be also be seen in the examples of the next section. Finally, the second-gradient homogenization procedure used in section 5 reveals that the effective reinforced plate structure would exhibit flexoelectric behavior (stress-field gradient or electric displacement-strain gradient) even if the constituents of the composite exhibited no flexoelectricity to begin with.

In the rest of this section, we will be concerned with obtaining the governing equations of the homogenized flexoelectric plate. To this end, we turn our attention to the first unit cell problem in equation (4.15b) which we multiply first by z and then by z^2 and then average the resulting expressions according to equation (3.12) to get,

$$\left\langle b_{i3}^{(1)\mu\nu}\right\rangle = \left\langle z b_{i3}^{(1)\mu\nu}\right\rangle = 0. \tag{6.3}$$

Repeating this procedure with the remaining unit cell problems in equations (4.15b) and (5.6) results in the following expressions:

$$\begin{aligned}
&\left\langle b_{i3}^{(1)\nu}\right\rangle = \left\langle z b_{i3}^{(1)\nu}\right\rangle = \left\langle B_{i3}^{*\mu\nu}\right\rangle = \left\langle z B_{i3}^{*\mu\nu}\right\rangle = \left\langle \delta_3^{(1)\mu\nu}\right\rangle = \left\langle z\delta_3^{(1)\mu\nu}\right\rangle = \\
&\qquad = \left\langle \delta_3^{(1)\nu}\right\rangle = \left\langle z\delta_3^{(1)\nu}\right\rangle = \left\langle \Delta_3^{*(f)\mu\nu}\right\rangle = \left\langle z\Delta_3^{*(f)\mu\nu}\right\rangle = 0 \\
&\left\langle B_{i3}^{\mu\nu\lambda}\right\rangle = \left\langle z b_{i\lambda}^{(1)\mu\nu}\right\rangle - \langle z\rangle\left\langle b_{i\lambda}^{(1)\mu\nu}\right\rangle, \quad \left\langle B_{i3}^{\nu\lambda}\right\rangle = \left\langle z b_{i\lambda}^{(1)\nu}\right\rangle - \langle z\rangle\left\langle b_{i\lambda}^{(1)\nu}\right\rangle \\
&\left\langle \Delta_3^{\mu\nu\lambda}\right\rangle = \left\langle z\delta_\lambda^{(1)\mu\nu}\right\rangle - \langle z\rangle\left\langle \delta_\lambda^{(1)\mu\nu}\right\rangle, \quad \left\langle \Delta_3^{(f)\nu\lambda}\right\rangle = \left\langle z\delta_\lambda^{(1)\nu}\right\rangle - \langle z\rangle\left\langle \delta_\lambda^{(1)\nu}\right\rangle.
\end{aligned} \tag{6.4}$$

We will make use of these expressions later on in this section. The asymptotic expansions in equations (5.10) and (5.11) essentially contain four macroscopic variables, v_1, v_2, w, and φ^*. To obtain the requisite system of equations for obtaining these variables, we refer to equation (4.1a) from which we write,

$$\left\langle H_\alpha^{(1)}\right\rangle + \delta H_\alpha^{(2)} = 0, \quad \left\langle H_3^{(1)}\right\rangle + \delta H_3^{(2)} + \delta^2 H_3^{(3)} = 0. \tag{6.5}$$

Averaging these expressions, applying the boundary conditions involving $\sigma_{ij}^{(1)}$, $\sigma_{ij}^{(2)}$, and $\sigma_{ij}^{(3)}$ from equation (4.1b) and using equation (6.2) results in the following equations:

$$\begin{aligned}
&\frac{\partial}{\partial x_\beta}\left(\left\langle b_{\alpha\beta}^{(1)\mu\nu}\right\rangle \varepsilon_{\mu\nu}^{(M)} + \left\langle b_{\alpha\lambda}^{(1)\nu}\right\rangle E_\nu^{(M)}\right) + \delta\frac{\partial}{\partial x_\beta}\left(\left\langle B_{\alpha\beta}^{*\mu\nu}\right\rangle \tau_{\mu\nu}^{(M)} + \left\langle B_{\alpha\beta}^{\mu\nu\lambda}\right\rangle \omega_{\mu\nu\lambda}^{(M)} + \left\langle B_{\alpha\beta}^{\mu\nu}\right\rangle V_{\mu\nu}^{(M)}\right) + \\
&+ \delta(\tilde{r}_\alpha(\boldsymbol{x}) + \langle f_\alpha\rangle) = 0 \quad \text{and} \\
&\left\langle \sigma_{3\beta}^{(1)}\right\rangle_{,\beta} + \delta\left\langle \sigma_{3\beta}^{(2)}\right\rangle_{,\beta} + \delta^2\left(\left\langle \sigma_{3\beta}^{(3)}\right\rangle_{,\beta} + \tilde{q}_3^*(\boldsymbol{x}) + \langle g_3^*\rangle\right) = 0,
\end{aligned} \tag{6.6}$$

where,

$$\begin{aligned}
&\tilde{r}_\alpha^*(\boldsymbol{x}) = \int_{-0.5}^{0.5}\int_{-0.5}^{0.5}\left(\omega^+ r_\alpha^{*+} + \omega^- r_\alpha^{*-}\right)dy_1dy_2, \quad \tilde{q}_3^*(\boldsymbol{x}) = \int_{-0.5}^{0.5}\int_{-0.5}^{0.5}\left(\omega^+ q_3^{*+} + \omega^- q_3^{*-}\right)dy_1dy_2, \\
&\tilde{r}_\alpha(\boldsymbol{x}) = \delta\tilde{r}_\alpha^*(\boldsymbol{x}), \quad \langle f_\alpha\rangle = \delta\langle f_\alpha^*\rangle.
\end{aligned} \tag{6.7}$$

The second expression in equation (6.6) is somewhat undesirable in that it involves $\left\langle \sigma_{3\beta}^{(3)}\right\rangle$ which we have not determined in the preceding analysis and would, therefore, like to eliminate. To this end, we return to the first expression in equation (6.5), multiply by z and average to obtain, on account of equations (4.1b) and (4.2a), an expression for $\left\langle \sigma_{3\beta}^{(3)}\right\rangle$ which we back-substitute into equation (6.6). After some algebraic manipulations and use of equation (6.4), we arrive at the desired expression in the form of,

$$\frac{\partial^2}{\partial x_\beta \partial x_\lambda}\left(\left\langle zb^{(1)\mu\nu}_{\beta\lambda}\right\rangle \varepsilon^{(M)}_{\mu\nu}+\left\langle zb^{(1)\nu}_{\beta\lambda}\right\rangle E^{(M)}_{\nu}\right)+\delta\frac{\partial^2}{\partial x_\alpha \partial x_\beta}\left(\langle z\rangle\left\langle B^{*\mu\nu}_{\alpha\beta}\right\rangle \tau^{(M)}_{\mu\nu}\right)+\delta q_3(\boldsymbol{x})$$
$$+\delta\frac{\partial^2}{\partial x_\alpha \partial x_\beta}\left(\left\langle zB^{\mu\nu\lambda}_{\alpha\beta}\right\rangle \omega^{(M)}_{\mu\nu\lambda}+\left\langle zB^{\mu\nu}_{\alpha\beta}\right\rangle V^{(M)}_{\mu\nu}\right)+\delta\frac{\partial}{\partial x_\beta}\left(\rho_\beta(\boldsymbol{x})+\left\langle zf_\beta\right\rangle\right)+\delta\langle g_3\rangle=0, \tag{6.8}$$

where,

$$\rho^*_\alpha(\boldsymbol{x})=\int_{-0.5}^{0.5}\int_{-0.5}^{0.5}\left(z^+\omega^+ r^{*+}_\alpha+z^-\omega^- r^{*-}_\alpha\right)dy_1dy_2,\quad \rho_\alpha=\rho^*_\alpha,\quad \tilde{q}_3=\delta q^*_3,\quad \langle g_3\rangle=\delta\left\langle g^*_3\right\rangle. \tag{6.9}$$

Turning, now, our attention to the electrical problem, we write from equation (4.1a),

$$\left\langle H^{*(1)}\right\rangle+\delta\left\langle H^{*(2)}\right\rangle=0. \tag{6.10}$$

Averaging this and making use of equations (3.13), (4.1b), and (6.2) results in,

$$\frac{\partial}{\partial x_\alpha}\left(\left\langle\delta^{(1)\mu\nu}_{\alpha}\right\rangle\varepsilon^{(M)}_{\mu\nu}+\left\langle\delta^{(1)\nu}_{\alpha}\right\rangle E^{(M)}_{\nu}\right)+\delta\frac{\partial}{\partial x_\alpha}\left(\left\langle\Delta^{*(f)\mu\nu}_{\alpha}\right\rangle\tau^{(M)}_{\mu\nu}+\langle\Delta^{\mu\nu\lambda}_{\alpha}\rangle\omega^{(M)}_{\mu\nu\lambda}+\langle\Delta^{\mu\nu}_{\alpha}\rangle V^{(M)}_{\mu\nu}\right)+$$
$$+\delta(\tilde{\sigma}(\boldsymbol{x})+\langle\rho\rangle)=0, \tag{6.11}$$

where,

$$\tilde{\sigma}^*(\boldsymbol{x})=\int_{-0.5}^{0.5}\int_{-0.5}^{0.5}(\omega^+\hat{\sigma}^+ +\omega^-\hat{\sigma}^-)dy_1dy_2,\quad \tilde{\sigma}=\delta\tilde{\sigma}^*,\quad \langle\rho\rangle=\delta\langle\hat{\rho}\rangle. \tag{6.12}$$

Thus, the first expression in equation (6.6) ($\alpha = 1, 2$) and equations (6.8) and (6.11) are the four requisite equations which, together with equations (3.2b) and (3.2d) can be used to determine the macroscopic variables v_1, v_2, w, and φ^*. To summarize, the microscopic problem entails solution of the unit cell problems in equations (4.15b) and (5.6) to obtain the local functions from which the coefficient functions are determined via equations (4.16) and (5.7a). These functions are then averaged on the basis of equation (3.12) to calculate the corresponding effective coefficients portrayed in equation (6.2). The macroscopic problem begins by substituting the expressions for the effective coefficients in equations (6.6), (6.8), and (6.11) to calculate v_1, v_2, w, and φ^* after which point all field variables such as mechanical stress, strain and strain gradient, electric displacement, field and field gradient, and so on can be obtained from equations (3.9a), (3.9b), (5.10), and (5.11).

7. Examples and discussion

The applicability of the model and the expressions of the effective coefficients will be illustrated in this section. The first example we consider consists of a laminated piezoelastic and flexoelectric plate, the unit cell of which is given in Figure 2. Clearly, the material properties are independent of y_1 and y_2, and all partial derivatives in the unit cell problems of equations (4.15b) and (5.6) as well the definitions of the coefficient functions in equations (4.16) and (5.7) become ordinary derivatives in z. We assume that the constituent materials exhibit a cubic crystal symmetry around the x_3 axis with the pertinent material tensors given in Appendix B, see Guinovart-Sanjuán et al. [24].

As shown in Figure 2, the layout of the laminate is completely governed by the parameters $\delta_0, \delta_1, \delta_2, ..., \delta_M$, where $\delta_0 = 0$, $\delta_M = 1$, and M corresponds to the number of laminae. The thickness of the mth layer is $\delta_m - \delta_{m-1}$ in this coordinate thickness while the real thickness as measured in the original $\{x_i\}$ coordinate system is $\delta(\delta_m - \delta_{m-1})$. Clearly, $\delta_m = z + 1/2$ and the normal vector $N_i = (0, 0, 1)$. Finally, it is readily determined that for a coefficient function $\mathbb{Q}_i$ which is constant in each lamina, the following formulae hold:

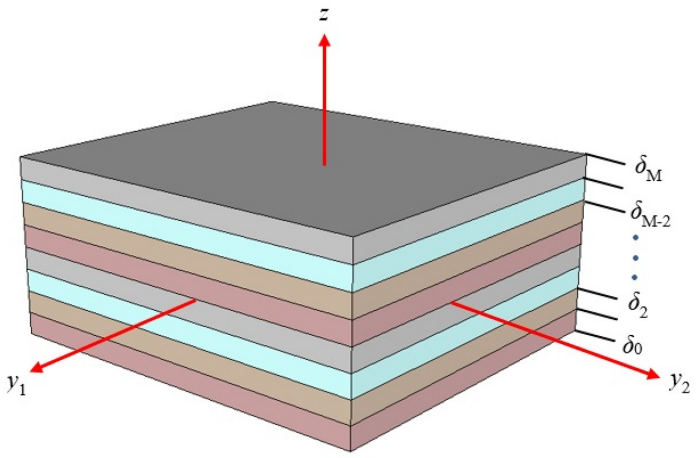

Figure 2. Periodic piezoelectric and flexoelectric composite laminate with M laminae.

$$\begin{aligned}
\langle \mathbb{Q}_i \rangle &= \int_{-0.5}^{0.5} \mathbb{Q}_i dz = \int_0^1 \mathbb{Q}_i d\delta_m = \sum_{m=1}^{M} \int_{\delta_{m-1}}^{\delta_m} \mathbb{Q}_i d\delta_m = \sum_{m=1}^{M} \mathbb{Q}_i^{(m)} (\delta_m - \delta_{m-1}) \\
\langle z\mathbb{Q}_i \rangle &= 1/2 \sum_{m=1}^{M} \mathbb{Q}_i^{(m)} \left[\delta_m^2 - \delta_{m-1}^2 - (\delta_m - \delta_{m-1}) \right], \\
\langle z^2\mathbb{Q}_i \rangle &= 1/3 \sum_{m=1}^{M} \mathbb{Q}_i^{(m)} \left[\delta_m^3 - \delta_{m-1}^3 - 3/2\left(\delta_m^2 - \delta_{m-1}^2\right) + 3/4(\delta_m - \delta_{m-1}) \right],
\end{aligned} \tag{7.1}$$

where $\mathbb{Q}_i^{(m)}$ is the value of the coefficient in the mth layer.

Let us now demonstrate the solution methodology for the unit cell problems, the determination of the local functions, and the final calculation of the effective coefficients. We will begin with the first and third unit cell problems in equation (4.15b) which, for the stratified structure of Figure 2, simplify to,

$$\begin{aligned}
b_{i3|3}^{(1)\mu\nu}(z) &= 0 & \delta_{3|3}^{(1)\mu\nu}(z) &= 0 \\
b_{i3}^{(1)\mu\nu}(z) &= 0 \quad \text{on } Z^{\pm} & \delta_{3}^{(1)\mu\nu}(z) &= 0 \quad \text{on } Z^{\pm}
\end{aligned} . \tag{7.2}$$

In each lamina, the solution of these differential equations and associated boundary conditions is straightforward, and is $b_{i3}^{(1)\mu\nu} = 0$ and $\delta_3^{(1)\mu\nu} = 0$. Using these results into the appropriate expressions for the function coefficients in equation (4.16) results in,

$$\begin{aligned}
b_{i3}^{(1)\mu\nu} &= c_{i3k3} N_{k|3}^{(1)\mu\nu} + e_{3i3} A_{|3}^{(1)\mu\nu} - \mu_{3i33}^{(f)} A_{|33}^{(1)\mu\nu} + c_{i3\mu\nu} = 0 \\
\delta_3^{(1)\mu\nu} &= e_{3k3} N_{k|3}^{(1)\mu\nu} + \mu_{3k33}^{(f)} N_{k|33}^{(1)\mu\nu} - \kappa_{11} A_{|3}^{(1)\mu\nu} + e_{3\mu\nu} = 0,
\end{aligned} \tag{7.3}$$

where the differential operators in equation (A.1) are also used. Letting index i assume values of 1, 2, or 3 in equation (7.3) leads to simple equations for the local functions $N_i^{(1)\mu\nu}$ and $A^{(1)\mu\nu}$, which yield the following expressions for the non-trivial solutions,

$$N_3^{(1)11} = N_3^{(1)22} = -\frac{c_{12}}{c_{11}} z, \quad A^{(1)12} = A^{(1)21} = \frac{e_{14}}{\kappa_{11}} z, \tag{7.4}$$

bearing in mind the material properties of equation (B.1). The analysis proceeds in much the same way for the remaining unit cell problems in equation (4.15b) giving the following solutions for the local functions:

$$\begin{aligned}
&M_1^{(1)1} = M_2^{(1)2} = M_3^{(1)\mu} = \Xi^{(1)\mu} = 0, \quad M_1^{(1)2} = M_2^{(1)1} = -\frac{e_{14}}{c_{66}} z \\
&N_3^{*(2)11} = N_3^{*(2)22} = \left(-c_{12}c_{11}^{-1}\right)\frac{z^2}{2}, \quad N_3^{*(2)12} = N_3^{*(2)21} = \left(\mu_{11}^{(f)} e_{14} c_{11}^{-1} \kappa_{11}^{-1}\right) z \\
&A^{*(2)11} = A^{*(2)22} = \left(\mu_{15}^{(f)} \kappa_{11}^{-1} - \mu_{11}^{(f)} c_{12} c_{11}^{-1} \kappa_{11}^{-1}\right) z, \quad A^{*(2)12} = A^{*(2)21} = \left(e_{14}\kappa_{11}^{-1}\right)\frac{z^2}{2} \\
&N_\alpha^{*(2)\mu\nu} = 0.
\end{aligned} \tag{7.5}$$

Using these local functions, function coefficients $b_{ij}^{(1)\mu\nu}$, $b_{ij}^{(1)\nu}$, $\delta_i^{(1)\mu\nu}$, $\delta_i^{(1)\nu}$, $B_{ij}^{*\mu\nu}$, and $\Delta_i^{*(f)\mu\nu}$ can be obtained from equation (4.16) and the corresponding effective coefficients be calculated on the basis of equation (7.1). The expressions for the effective coefficients will be given in the sequel.

Turning our attention to the unit cell problems stemming from second-gradient homogenization, we begin with the first and third expressions in equation (5.6) which reduce to,

$$\begin{aligned}
&b_{i\lambda}^{(1)\mu\nu} - \left\langle b_{i\lambda}^{(1)\mu\nu} \right\rangle + B_{i3|3}^{\mu\nu\lambda} = 0 \qquad && \delta_\lambda^{(1)\mu\nu} - \left\langle \delta_\lambda^{(1)\mu\nu} \right\rangle + \Delta_{3|3}^{\mu\nu\lambda} = 0 \\
&B_{i3}^{\mu\nu\lambda} = 0 \quad on\ Z^{\pm} && \Delta_3^{\mu\nu\lambda} = 0 \quad on\ Z^{\pm}
\end{aligned}. \tag{7.6}$$

Considering the first of the foregoing expressions results in the following expression in each lamina,

$$B_{i3}^{\mu\nu\lambda} = \left\langle b_{i\lambda}^{(1)\mu\nu} \right\rangle z - b_{i\lambda}^{(1)\mu\nu} z + \mathbb{C}_i^{\mu\nu\lambda}, \tag{7.7}$$

where $\mathbb{C}_i^{\mu\nu\lambda}$ are constants of integration which are obtained in each lamina to satisfy the second set of continuity conditions in equation (5.8). Letting, as an example, indices $i, \mu, \nu, \lambda = 1, 1, 1, 1$ and substituting equation (7.7) into equation (5.7) results, on account of equation (7.4), in the following expression:

$$N_1^{(2)111} = \left(c_{12}c_{11}^{-1} + \left\langle b_{11}^{(1)11} \right\rangle c_{66}^{-1} - b_{11}^{(1)11} c_{66}^{-1}\right)\frac{z^2}{2} + \mathbb{C}_1^{111} c_{66}^{-1} z. \tag{7.8}$$

The remaining $N_i^{(2)\mu\nu\lambda}$ local functions as well as their $A^{\mu\nu\lambda}$ counterparts are obtained in a similar fashion. It is important to note that since we are dealing with a fully coupled problem, the local functions for some index combinations, e.g., $i, \mu, \nu, \lambda = 3, 1, 1, 1$ must be obtained from both unit cells in equation (7.6) as a system. In other words, we obtain two equations in $N_3^{(2)111}$ and A^{111} which must be solved simultaneously. The final expressions for the local functions are given below:

$$\begin{aligned}
&N_1^{(2)111} = N_2^{(2)222} = \left(c_{12}c_{11}^{-1} + \left\langle b_{11}^{(1)11} \right\rangle c_{66}^{-1} - b_{11}^{(1)11} c_{66}^{-1}\right)\frac{z^2}{2} + \left(\mathbb{C}_1^{111} c_{66}^{-1}\right) z \\
&N_2^{(2)112} = N_1^{(2)221} = \left(c_{12}c_{11}^{-1} + \left\langle b_{22}^{(1)11} \right\rangle c_{66}^{-1} - b_{22}^{(1)11} c_{66}^{-1}\right)\frac{z^2}{2} + \left(\mathbb{C}_2^{112} c_{66}^{-1}\right) z \\
&N_1^{(2)121} = N_1^{(2)211} = N_2^{(2)122} = N_2^{(2)211} = N_2^{(2)212} = \left(2\mu_{46}^{(f)} e_{14} c_{66}^{-1} \kappa_{11}^{-1}\right) z \\
&N_2^{(2)121} = N_1^{(2)122} = N_1^{(2)212} = \left(\left\langle b_{12}^{(1)12} \right\rangle c_{66}^{-1} - b_{12}^{(1)12} c_{66}^{-1} - e_{14}^2 c_{66}^{-1} \kappa_{11}^{-1}\right)\frac{z^2}{2} + \left(\mathbb{C}_1^{122} c_{66}^{-1}\right) z \\
&N_2^{(2)111} = N_1^{(2)112} = N_2^{(2)221} = N_1^{(2)222} = N_3^{(2)\mu\nu\lambda} = A^{(2)\mu\nu\lambda} = 0.
\end{aligned} \tag{7.9}$$

Substitution of equation (7.5) into equation (4.8) reveals that $b_{i\lambda}^{(1)\nu}=0$ so that the second and fourth unit cell problems in equation (5.6) become,

$$\begin{array}{ll} B_{i3|3}^{\nu\lambda}=0 & \delta_{\lambda}^{(1)\nu}-\left\langle\delta_{\lambda}^{(1)\nu}\right\rangle+\Delta_{3|3}^{(f)\nu\lambda}=0 \\ B_{i3}^{\nu\lambda}=0 \quad on\ Z^{\pm} & \Delta_{3}^{(f)\nu\lambda}=0 \quad on\ Z^{\pm} \end{array}. \tag{7.10}$$

The solutions of these problems may be written down as,

$$B_{i3}^{\nu\lambda}=0, \quad \Delta_{3}^{(f)\nu\lambda}=\left\langle\delta_{\lambda}^{(1)\nu}\right\rangle z-\delta_{\lambda}^{(1)\nu}z+\mathbb{C}^{(f)\nu\lambda}, \tag{7.11}$$

where $\mathbb{C}^{(f)\nu\lambda}$, much like their $\mathbb{C}_{i}^{\mu\nu\lambda}$ counterparts in equation (7.7), are constants of integration that must be calculated in each lamina to satisfy the interface conditions, see equation (5.8). Solution of equation (7.11) in combination with the pertinent expressions in equation (5.7) gives the relevant local functions in the form of,

$$\begin{aligned} M_{3}^{(2)11}&=M_{3}^{(2)22}=\left(\mu_{15}^{(f)}c_{11}^{-1}+\mu_{11}^{(f)}\delta_{1}^{1}c_{11}^{-1}\kappa_{11}^{-1}-\mu_{11}^{(f)}\langle\delta_{1}^{1}\rangle c_{11}^{-1}\kappa_{11}^{-1}-\mu_{11}^{(f)}e_{14}^{2}c_{11}^{-1}c_{66}^{-1}\kappa_{11}^{-1}\right)z \\ M_{3}^{(2)12}&=M_{3}^{(2)21}=\left(e_{14}c_{12}c_{11}^{-1}c_{66}^{-1}\right)\frac{z^{2}}{2}, \quad M_{\alpha}^{(2)\mu\nu}=0 \\ \Xi^{(2)11}&=\Xi^{(2)22}=\left(\delta_{1}^{1}\kappa_{11}^{-1}-\langle\delta_{1}^{1}\rangle\kappa_{11}^{-1}-e_{14}^{2}c_{66}^{-1}\kappa_{11}^{-1}\right)\frac{z^{2}}{2}-\left(\mathbb{C}^{(f)22}\kappa_{11}^{-1}\right)z \\ \Xi^{(2)12}&=\Xi^{(2)21}=\left(\mu_{11}^{(f)}e_{14}c_{12}c_{11}^{-1}c_{66}^{-1}\kappa_{11}^{-1}-\left[\mu_{46}^{(f)}+\mu_{15}^{(f)}\right]e_{14}c_{66}^{-1}\kappa_{11}^{-1}\right)z. \end{aligned} \tag{7.12}$$

An important point needs to be made with regard to the local functions given in this section. In particular, they are unique up to constant terms, an ambiguity which can be removed, see Kalamkarov [49], by imposing that their average with respect to y_1 and y_2 only, $\langle\ldots\rangle_y$, vanishes when $z=0$. In other words, for an arbitrary local function, $\mathbb{N}_{ij\ldots}^{\mu\nu\ldots}$, we impose that,

$$\left\langle\mathbb{N}_{ij\ldots}^{\mu\nu\ldots}\right\rangle_{y}=0 \text{ when } z=0. \tag{7.13}$$

Thus, for a laminate with M laminae, there are M constants that must be found. $M-1$ equations will be obtained from as many interface conditions as dictated by the first expression in equation (5.8) and the last requisite equation will come from equation (7.14). However, we do not bother calculating these constants because all coefficient functions contain derivatives of the local functions. Consequently, neither the coefficient functions nor the effective coefficients will be affected by these constants, and hence they do not show up in equations (7.4), (7.5), (7.9), and (7.12).

With equations (4.16), (5.7), (6.2), and (7.1) in mind, we are now ready to compute the effective coefficients for the stratified structure of Figure 2. The effective extensional, $\delta\left\langle b_{\alpha\beta}^{(1)\nu\lambda}\right\rangle$, bending, $\delta^{3}\left\langle zB_{\alpha\beta}^{*\nu\lambda}\right\rangle$, and coupling, $\delta^{2}\left\langle zb_{\alpha\beta}^{(1)\nu\lambda}\right\rangle$, $\delta^{2}\left\langle B_{\alpha\beta}^{*\nu\lambda}\right\rangle$, elastic coefficients are given by,

$$\begin{aligned} &\left\langle b_{11}^{(1)11}\right\rangle=\left\langle b_{22}^{(1)22}\right\rangle=\langle c_{11}-c_{12}^{2}c_{11}^{-1}\rangle, \quad \left\langle b_{22}^{(1)11}\right\rangle=\left\langle b_{11}^{(1)22}\right\rangle=\langle c_{12}-c_{12}^{2}c_{11}^{-1}\rangle \\ &\left\langle b_{12}^{(1)12}\right\rangle=\langle c_{66}+e_{14}^{2}\kappa_{11}^{-1}\rangle, \quad \left\langle zb_{11}^{(1)11}\right\rangle=\left\langle zb_{22}^{(1)22}\right\rangle=\langle(c_{11}-c_{12}^{2}c_{11}^{-1})z\rangle \\ &\left\langle zb_{22}^{(1)11}\right\rangle=\left\langle zb_{11}^{(1)22}\right\rangle=\langle(c_{12}-c_{12}^{2}c_{11}^{-1})z\rangle \\ &\left\langle zb_{12}^{(1)12}\right\rangle=\langle(c_{66}+e_{14}^{2}\kappa_{11}^{-1})z\rangle, \quad \delta^{2}\langle B_{11}^{*11}\rangle=\delta^{2}\langle B_{22}^{*22}\rangle=\delta^{2}\langle(c_{11}-c_{12}^{2}c_{11}^{-1})z\rangle \\ &\langle B_{12}^{*12}\rangle=\langle(c_{66}+e_{14}^{2}\kappa_{11}^{-1})z\rangle, \quad \delta^{2}\langle B_{12}^{*11}\rangle=\delta\langle e_{14}(\mu_{15}\kappa_{11}^{-1}-\mu_{11}c_{12}c_{11}^{-1}\kappa_{11}^{-1})\rangle \\ &\langle zB_{11}^{*11}\rangle=\langle zB_{22}^{*22}\rangle=\langle(c_{11}-c_{12}^{2}c_{11}^{-1})z^{2}\rangle, \quad \delta^{2}\langle zB_{12}^{*11}\rangle=\delta\langle e_{14}(\mu_{15}\kappa_{11}^{-1}-\mu_{11}c_{12}c_{11}^{-1}\kappa_{11}^{-1})z\rangle \\ &\langle zB_{12}^{*12}\rangle=\langle(c_{66}+e_{14}^{2}\kappa_{11}^{-1})z^{2}\rangle, \quad \delta^{2}\langle zB_{11}^{*12}\rangle=\delta\langle e_{14}(\mu_{11}c_{12}c_{11}^{-1}\kappa_{11}^{-1}-\mu_{15}\kappa_{11}^{-1})z\rangle. \end{aligned} \tag{7.14}$$

The effective in-plane, $\delta\left\langle b_{\alpha\beta}^{(1)\nu}\right\rangle$, $\delta\left\langle \delta_i^{(1)\nu\lambda}\right\rangle$, and out-of-plane, $\delta\left\langle zb_{\alpha\beta}^{(1)\nu}\right\rangle$, piezoelectric coefficients as well as the effective dielectric permittivity constants, $-\delta\left\langle \delta_i^{(1)\nu}\right\rangle$ by,

$$\left\langle b_{\alpha\beta}^{(1)\nu}\right\rangle = \left\langle \delta_i^{(1)\mu\nu}\right\rangle = \left\langle zb_{\alpha\beta}^{(1)\nu}\right\rangle = 0, \quad -\left\langle \delta_1^{(1)1}\right\rangle = -\left\langle \delta_2^{(1)2}\right\rangle = \left\langle \kappa_{11} + e_{14}^2 c_{66}^{-1}\right\rangle. \tag{7.15}$$

Clearly, choosing different crystal geometries or materials with different poling directions would have yielded entirely different results; this shows an advantage of the developed model in that it can be used to tailor the effective properties of a given structure by changing geometrical (e.g., stacking sequence or relative volume fractions in the case of laminates), physical (e.g., poling direction), or material (e.g., constituent properties) parameter of interest.

The in-plane and out-of-plane strain gradient effective elastic coefficients, $\delta^2\left\langle B_{ij}^{\mu\nu\lambda}\right\rangle$ and $\delta^2\left\langle zB_{\alpha\beta}^{\mu\nu\lambda}\right\rangle$, the electric displacement-field gradient coupling coefficients, $-\delta^2\left\langle \Delta_i^{(f)\nu\lambda}\right\rangle$, and the electric displacement-curvature coupling coefficients, $-\delta^2\left\langle \Delta_i^{*(f)\nu\lambda}\right\rangle$, are given by,

$$\begin{aligned}
&\left\langle B_{13}^{111}\right\rangle = \left\langle B_{23}^{222}\right\rangle = \left\langle \left(c_{11} - c_{12}^2 c_{11}^{-1}\right)z\right\rangle, \quad \left\langle B_{13}^{122}\right\rangle = \left\langle B_{23}^{211}\right\rangle = \left\langle \left(c_{66} + e_{14}^2\kappa_{11}^{-1}\right)z\right\rangle \\
&\left\langle B_{13}^{221}\right\rangle = \left\langle B_{23}^{112}\right\rangle = \left\langle \left(c_{12} - c_{12}^2 c_{11}^{-1}\right)z\right\rangle, \quad \left\langle zB_{\alpha\beta}^{\mu\nu\lambda}\right\rangle = 0 \\
&-\left\langle \Delta_3^{(f)11}\right\rangle = -\left\langle \Delta_3^{(f)22}\right\rangle = \left\langle \left(\kappa_{11} + e_{14}^2 c_{66}^{-1}\right)z\right\rangle, \quad \left\langle \Delta_\alpha^{(f)\nu\lambda}\right\rangle = \left\langle \Delta_\alpha^{*(f)\nu\lambda}\right\rangle = 0.
\end{aligned} \tag{7.16}$$

Next, the in-plane effective flexoelectric coefficients, $-\delta^2\left\langle B_{ij}^{\mu\nu}\right\rangle$, $\delta^2\left\langle \Delta_i^{\mu\nu\lambda}\right\rangle$ are given by,

$$\begin{aligned}
\delta^2\left\langle B_{11}^{11}\right\rangle &= \delta^2\left\langle B_{22}^{22}\right\rangle = \delta\left\langle c_{12}c_{11}^{-1}(\mu_{15} - \mu_{11})\right\rangle + 2\delta\left\langle e_{14}^2\kappa_{11}^{-1}c_{66}^{-1}\left(\mu_{15} - \mu_{11}c_{12}c_{11}^{-1}\right)\right\rangle + \\
&\quad - \delta\left\langle \kappa_{11} + e_{14}^2 c_{66}^{-1}\right\rangle\left[\left\langle \mu_{15}\kappa_{11}^{-1} - \mu_{11}c_{12}c_{11}^{-1}\kappa_{11}^{-1}\right\rangle\right] + \delta\left\langle \mu_{15} - \mu_{11}\right\rangle \\
\left\langle B_{11}^{12}\right\rangle &= \left\langle B_{22}^{21}\right\rangle = \left\langle e_{14}c_{66}^{-1}\left(c_{12}^2c_{11}^{-1} - c_{12}\right)z\right\rangle, \quad \left\langle B_{11}^{21}\right\rangle = \left\langle B_{22}^{12}\right\rangle = \left\langle e_{14}c_{66}^{-1}\left(c_{12}^2c_{11}^{-1} - c_{11}\right)z\right\rangle \\
\left\langle B_{12}^{11}\right\rangle &= \left\langle B_{12}^{22}\right\rangle = \left\langle \kappa_{11} + e_{14}^2c_{66}^{-1}\right\rangle\left\langle e_{14}\kappa_{11}^{-1}z\right\rangle - 2\left\langle e_{14}z\right\rangle - 2\left\langle e_{14}^3\kappa_{11}^{-1}c_{66}^{-1}z\right\rangle - \left\langle e_{14}^2\kappa_{11}^{-1}\mathbb{C}^{(f)11}\right\rangle \\
\delta^2\left\langle B_{11}^{22}\right\rangle &= \delta^2\left\langle B_{22}^{11}\right\rangle = \delta\left\langle c_{12}c_{11}^{-1}(\mu_{15} - \mu_{11})\right\rangle + 2\delta\left\langle e_{14}^2\kappa_{11}^{-1}c_{66}^{-1}\left(\mu_{15} - \mu_{11}c_{12}c_{11}^{-1}\right)\right\rangle + \\
&\quad - \delta\left\langle \kappa_{11} + e_{14}^2c_{66}^{-1}\right\rangle\left[\left\langle \mu_{15}\kappa_{11}^{-1} - \mu_{11}c_{12}c_{11}^{-1}\kappa_{11}^{-1}\right\rangle\right] \\
\delta^2\left\langle B_{12}^{12}\right\rangle &= \delta^2\left\langle B_{12}^{21}\right\rangle = \delta\left\langle \mu_{11}e_{14}^2c_{12}\kappa_{11}^{-1}c_{11}^{-1}c_{66}^{-1}\right\rangle - \delta\left\langle e_{14}^2\kappa_{11}^{-1}c_{66}^{-1}(\mu_{46} + \mu_{15})\right\rangle - \delta\left\langle \mu_{46}\right\rangle,
\end{aligned} \tag{7.17a}$$

and,

$$\begin{aligned}
\delta^2\left\langle \Delta_1^{111}\right\rangle &= \delta^2\left\langle \Delta_2^{222}\right\rangle = \delta\left\langle \mu_{46}c_{66}^{-1}\right\rangle\left\langle c_{11} - c_{12}^2c_{11}^{-1}\right\rangle - \delta\left\langle \mu_{46}c_{66}^{-1}\left(c_{11} - c_{12}^2c_{11}^{-1}\right)\right\rangle + \\
&\quad + \delta\left\langle \mu_{11} - \mu_{15}c_{12}c_{11}^{-1}\right\rangle \\
\left\langle \Delta_1^{112}\right\rangle &= \left\langle \Delta_2^{211}\right\rangle = \left\langle c_{12} - c_{12}^2c_{11}^{-1}\right\rangle\left\langle e_{14}c_{66}^{-1}z\right\rangle - \left\langle \left(c_{12} - c_{12}^2c_{11}^{-1}\right)e_{14}c_{66}^{-1}z\right\rangle + \left\langle e_{14}c_{66}^{-1}\mathbb{C}_2^{112}\right\rangle \\
\left\langle \Delta_1^{121}\right\rangle &= \left\langle \Delta_1^{211}\right\rangle = \left\langle e_{14}^2\kappa_{11}^{-1} + c_{66}\right\rangle\left\langle e_{14}c_{66}^{-1}z\right\rangle - 2\left\langle e_{14}z\right\rangle - 2\left\langle e_{14}^3\kappa_{11}^{-1}c_{66}^{-1}z\right\rangle + \left\langle e_{14}c_{66}^{-1}\mathbb{C}_2^{121}\right\rangle \\
\delta^2\left\langle \Delta_1^{212}\right\rangle &= \delta^2\left\langle \Delta_2^{121}\right\rangle = \delta\left\langle \mu_{46}c_{66}^{-1}\right\rangle\left\langle e_{14}^2\kappa_{11}^{-1} + c_{66}\right\rangle + \delta\left\langle \mu_{15} - \mu_{46}\right\rangle \\
\delta^2\left\langle \Delta_1^{221}\right\rangle &= \delta^2\left\langle \Delta_1^{112}\right\rangle = \delta\left\langle \mu_{46}c_{66}^{-1}\right\rangle\left\langle c_{12} - c_{12}^2c_{11}^{-1}\right\rangle - \delta\left\langle \mu_{46}c_{66}^{-1}\left(c_{12} - c_{12}^2c_{11}^{-1}\right)\right\rangle + \\
&\quad + \delta\left\langle \mu_{46} - \mu_{15}c_{12}c_{11}^{-1}\right\rangle \\
\left\langle \Delta_1^{222}\right\rangle &= \left\langle \Delta_2^{111}\right\rangle = \left\langle c_{11} - c_{12}^2c_{11}^{-1}\right\rangle\left\langle e_{14}c_{66}^{-1}z\right\rangle - \left\langle \left(c_{11} - c_{12}^2c_{11}^{-1}\right)e_{14}c_{66}^{-1}z\right\rangle + \left\langle e_{14}c_{66}^{-1}\mathbb{C}_2^{222}\right\rangle.
\end{aligned} \tag{7.17b}$$

Finally, the out-of-plane effective flexoelectric coefficients, $-\delta^3\left\langle zB_{ij}^{\mu\nu}\right\rangle$, coupling moment resultants with field gradient are given in equation (7.17c):

$$
\begin{aligned}
\delta^3\langle zB_{11}^{11}\rangle &= \delta^2\langle c_{12}c_{11}^{-1}(\mu_{15}-\mu_{11})z\rangle + 2\delta^2\langle e_{14}^2\kappa_{11}^{-1}c_{66}^{-1}(\mu_{15}-\mu_{11}c_{12}c_{11}^{-1})z\rangle + \\
&\quad - \delta^2\langle \kappa_{11}+e_{14}^2c_{66}^{-1}\rangle\langle(\mu_{15}\kappa_{11}^{-1}-\mu_{11}c_{12}c_{11}^{-1}\kappa_{11}^{-1})z\rangle + \delta^2\langle(\mu_{15}-\mu_{11})z\rangle \\
\langle zB_{11}^{12}\rangle &= \langle zB_{22}^{21}\rangle = \langle e_{14}c_{66}^{-1}(c_{12}^2c_{11}^{-1}-c_{12})z^2\rangle \\
\langle zB_{11}^{21}\rangle &= \langle zB_{22}^{12}\rangle = \langle e_{14}c_{66}^{-1}(c_{12}^2c_{11}^{-1}-c_{11})z^2\rangle \\
\langle zB_{12}^{11}\rangle &= \langle zB_{12}^{22}\rangle = \langle \kappa_{11}+e_{14}^2c_{66}^{-1}\rangle\langle e_{14}\kappa_{11}^{-1}z^2\rangle - 2\langle e_{14}z^2\rangle - 2\langle e_{14}^3\kappa_{11}^{-1}c_{66}^{-1}z^2\rangle + \\
&\quad - \left\langle e_{14}^2\kappa_{11}^{-1}\mathbb{C}^{(f)11}z\right\rangle \\
\delta^3\langle zB_{11}^{22}\rangle &= \delta^2\langle c_{12}c_{11}^{-1}(\mu_{15}-\mu_{11})z\rangle + 2\delta^2\langle e_{14}^2\kappa_{11}^{-1}c_{66}^{-1}(\mu_{15}-\mu_{11}c_{12}c_{11}^{-1})z\rangle + \\
&\quad - \delta^2\langle \kappa_{11}+e_{14}^2c_{66}^{-1}\rangle\langle(\mu_{15}\kappa_{11}^{-1}-\mu_{11}c_{12}c_{11}^{-1}\kappa_{11}^{-1})z\rangle \\
\delta^3\langle zB_{12}^{12}\rangle &= \delta^3\langle zB_{12}^{21}\rangle = \delta^2\langle(\mu_{11}e_{14}^2c_{12}\kappa_{11}^{-1}c_{11}^{-1}c_{66}^{-1})z\rangle - \delta^2\langle e_{14}^2\kappa_{11}^{-1}c_{66}^{-1}(\mu_{46}+\mu_{15})z\rangle + \\
&\quad - \delta^2\langle z\mu_{46}\rangle.
\end{aligned}
\tag{7.17c}
$$

We note that if we ignore the flexoelectric effect, the expressions for the effective elastic, piezoelectric, and dielectric coefficients in equations (7.14) and (7.15) match those in Hadjiloizi et al. [40] and if we further ignore piezoelectric and dielectric effects, then the effective elastic coefficients (extensional, bending, coupling) conform to those in Kalamkarov et al. [49] as well as their counterparts obtained via the classical composite laminate theory, see, for example, Gibson [73] and Reddy [74]. As a numerical example of the foregoing work, let us consider a 1 mm thick four-layered antisymmetric laminate consisting of $BaTiO_3$ and GaAs with $BaTiO_3$ occupying the top-layer position and GaAs the bottom-layer position. The material properties of the two constituents are given in Guinovart-Sanjuán et al. [24].

Let us suppose that we vary the thickness of the GaAs layers from 0 to 0.5 mm which is tantamount to its volume fraction changing from 0 to 1. Figure 3 shows two typical out-of-plane flexoelectric coefficients, $\langle zB_{12}^{12}\rangle$ and $\langle zB_{11}^{12}\rangle$, normalized with respect to the maximum value in each case. Recall from equation (6.2) that these coefficients couple the moment resultants, $M_{12}^{(f)}$ and $M_{11}^{(f)}$ with the gradient of the electric potential ($\varphi_{,12}^{(0)}$ and $\varphi_{,11}^{(0)}$, respectively). As seen in Figure 3, $\langle zB_{12}^{12}\rangle$ peaks when the two constituents have equal volume fractions and drops to zero when the laminate becomes symmetric at a GaAs volume fraction of either 0 or 1. On the contrary, $\langle zB_{11}^{12}\rangle$ peaks when this volume fraction is 1 due to a higher value of B_{11}^{12} for GaAs as compared to that for $BaTiO_3$. Figure 4 shows the variation of the effective $\left\langle z\Delta_3^{(f)22}\right\rangle$ coefficient, which couples electric displacement with the gradient of the electric field, and

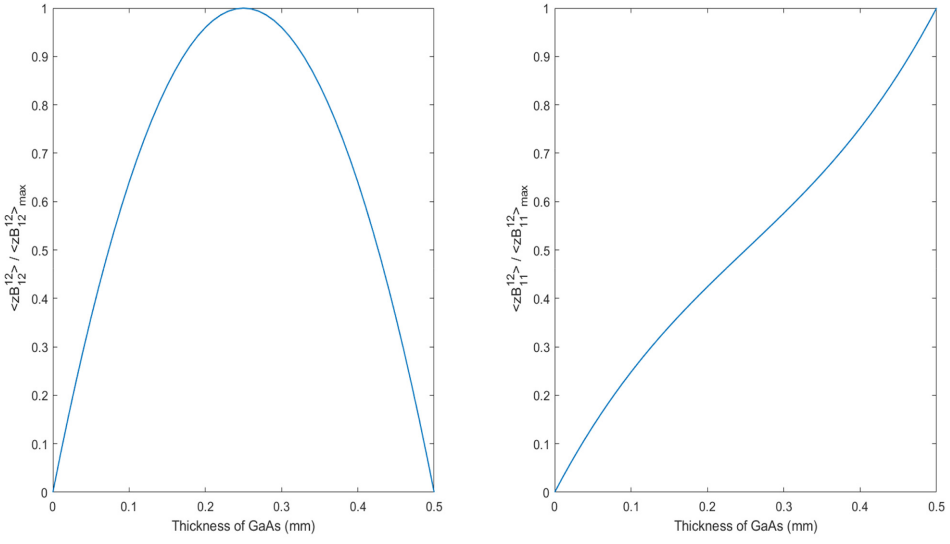

Figure 3. Plot of the effective $\langle zB_{12}^{12}\rangle$ and $\langle zB_{11}^{12}\rangle$ flexoelectric coefficients vs. thickness of the GaAs laminae.

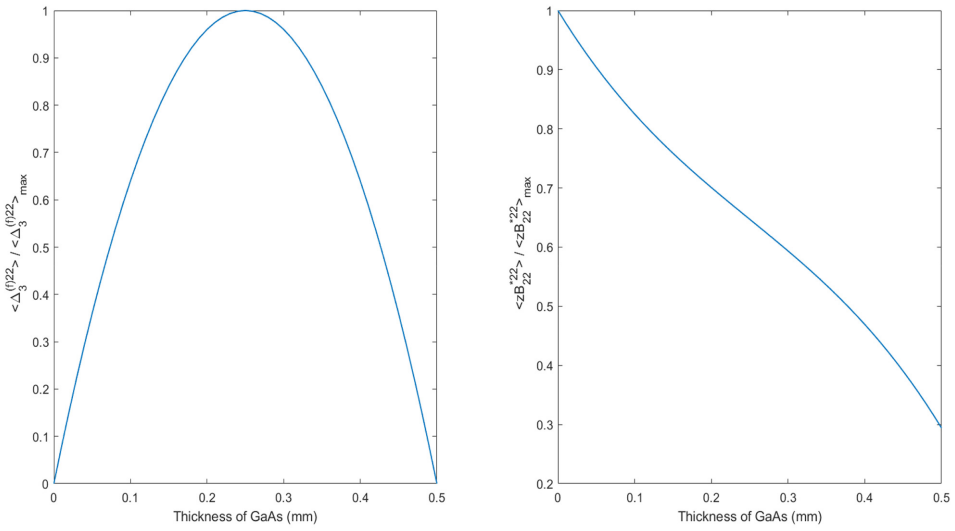

Figure 4. Plot of the effective $\left\langle z\Delta_3^{(f)22}\right\rangle$ and $\left\langle zB_{22}^{*22}\right\rangle$ coefficients vs. thickness of the GaAs laminae.

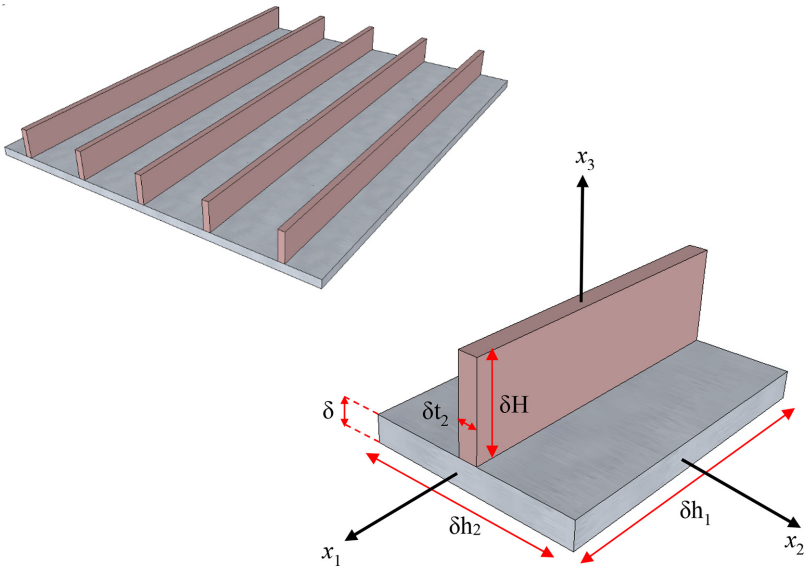

Figure 5. Flexoelectric ribbed plate and its unit cell in the macroscopic variables.

the effective bending stiffness in the x_2 direction, $\left\langle zB_{22}^{*22}\right\rangle$, vs. the thickness of the GaAs constituent. It is seen that $\left\langle z\Delta_3^{(f)22}\right\rangle$ peaks when the two constituents have equal volume fractions and the elastic coefficient peaks when the entire laminate is made of $BaTiO_3$ since this material is stiffer than its GaAs counterpart. Clearly all these trends can be changed by changing a geometrical (e.g., stacking configuration), material (nature of constituents), or physical (e.g., poling direction) parameter of interest. The closed-form expressions obtained in this work afford complete flexibility in this manner and allow customization of the effective properties of the laminate according to the requirements of a particular application.

The second example we will examine here pertains to the ribbed flexoelectric plate of Figure 5. The second-gradient unit cell problems in equation (5.6) have not yet been solved for this geometry and will not be considered in this work. Furthermore, to reduce the complexity of the relevant calculations we will exclude the influence of the flexoelectric effect and so the first four unit cell problems in equation

(4.15b) reduce to those in equation (4.7) and $b_{ij}^{(1)\mu\nu}$, $b_{ij}^{(1)\nu}$, $\delta_i^{(1)\mu\nu}$, *and* $\delta_i^{(1)\mu\nu}$ reduce to $b_{ij}^{\mu\nu}$, b_{ij}^{ν}, $\delta_i^{\mu\nu}$, and $\delta_i^{\mu\nu}$.

Consequently, let us examine the first and third unit cell problems in equation (4.7) which we express as,

$$\begin{array}{ll} \dfrac{1}{h_\gamma}\tau_{i\gamma|\gamma}^{\mu\nu}(\boldsymbol{y},z)+\tau_{i3|3}^{\mu\nu}(\boldsymbol{y},z)=0 & \dfrac{1}{h_\mu}\pi_{\gamma|\gamma}^{\mu\nu}(\boldsymbol{y},z)+\pi_{3|3}^{\mu\nu}(\boldsymbol{y},z)=0 \\ \dfrac{1}{h_\gamma}\tau_{i\gamma}^{\mu\nu}(\boldsymbol{y},z)n_\gamma^{\pm}+\tau_{i3}^{\mu\nu}n_3^{\pm}=0 \quad \textit{on } Z^{\pm} & \dfrac{1}{h_\gamma}\pi_{\gamma}^{k\nu}(\boldsymbol{y},z)n_\gamma^{\pm}+\pi_{3}^{\mu\nu}n_3^{\pm}=0 \quad \textit{on } Z^{\pm} \end{array}, \tag{7.18a}$$

where $n_i^{\pm}$ are the y_i components of the normal vector and,

$$\tau_{ij}^{\mu\nu}=b_{ij}^{\mu\nu}-c_{ij\mu\nu}, \quad \pi_i^{\mu\nu}=\delta_i^{\mu\nu}+e_{i\mu\nu}. \tag{7.18b}$$

We will follow the same methodology as the one we adopted in our previous work, see, for example, Hadjiloizi et al. [55], and obtain the local functions, coefficient functions, and effective coefficients in the rib and in the plate separately, and then superimpose the results. We will illustrate this methodology by solving the preceding unit cell problems for index combination $\mu,\nu=1,1$. We reiterate that the unit cell problems are defined in terms of the microscopic variables, and their solution is carried out in this domain. In view of equation (3.3), it is clear that, with respect to the microscopic variables, the plate is defined by $-1/2<y_1<1/2$, $-1/2<y_2<1/2$, and $-1/2<z<1/2$, while the rib is defined by $-1/2<y_1<1/2$, $-t_2/2h_2<y_2<t_2/2h_2$, and $-1/2<z<1/2+H$. Periodicity considerations stipulate that boundary conditions on the plate must be specified on $z=\pm1/2$ (where $n_1=n_2=0$, $n_3=1$), while in the region of the rib, they must be specified on $y_2=\pm t_2/2h_2$ (where $n_1=n_3=0$, $n_2=1$), and $z=1/2,\ 1/2+H$. Examination of equation (7.18a) as well as the relevant expressions in equation (4.8) reveals that these boundary conditions take the following form:

$$\begin{array}{l} \tau_{13}^{11}=\tau_{23}^{11}=0, \ \ \tau_{33}^{11}=-c_{12}, \quad \pi_3^{11}=-e_{31} \text{ on } z=\pm1/2 \text{ in plate} \\ \tau_{12}^{11}=\tau_{23}^{11}=0, \ \ \tau_{22}^{11}=-c_{12}, \quad \pi_2^{11}=0 \text{ on } y_2=\pm t_2/2h_2 \text{ in rib} \\ \tau_{13}^{11}=\tau_{23}^{11}=0, \ \ \tau_{33}^{11}=-c_{12}, \quad \pi_3^{11}=-e_{31} \text{ on } z=1/2,\ 1/2+H \text{ in rib}. \end{array} \tag{7.18c}$$

Periodicity in y_1 and y_2 in the region of the plate simplifies the governing equations in equation (7.18a) to $\tau_{i3|3}^{\mu\nu}=0$ and $\pi_{3|3}^{\mu\nu}=0$ in which we substitute the relevant expressions from equation (4.8) to give, on account of equations (7.18b) and (7.18c), the following solutions for the local functions N_3^{11} and A^{11}:

$$N_3^{11}=-c_{13}c_{33}^{-1}z, \quad A^{11}=0. \tag{7.19a}$$

Moving now to the region of the rib, we notice that since it is oriented entirely in the y_1 direction, we have no dependency on y_1 so that the pertinent expressions in equation (7.19a) become:

$$\frac{1}{h_2}\tau_{i2|2}^{\mu\nu}(\boldsymbol{y},z)+\tau_{i3|3}^{\mu\nu}(\boldsymbol{y},z)=0, \quad \frac{1}{h_\mu}\pi_{2|2}^{\mu\nu}(\boldsymbol{y},z)+\pi_{3|3}^{\mu\nu}(\boldsymbol{y},z)=0. \tag{7.19b}$$

Substitution of equation (4.8) into equation (7.19b) gives, on account of equations (7.18b) and (7.18c), a system of three equations in the local functions N_2^{11},N_3^{11},A^{11}, the solution of which is straightforward and is:

$$N_2^{11}=h_2\left(c_{12}^2-c_{12}c_{11}\right)\left(c_{11}^2-c_{12}^2\right)^{-1}y_2, \quad N_3^{11}=\left(c_{12}^2-c_{12}c_{11}\right)\left(c_{11}^2-c_{12}^2\right)^{-1}z, \quad A^{11}=0. \tag{7.20}$$

Back substitution of equation (7.20) into equation (4.8) gives the desired expressions for the coefficient functions in the form of,

$$b_{11}^{11(p)}=c_{11}-c_{12}^2c_{11}^{-1}, \quad b_{11}^{11(r)}=c_{11}+2\left(c_{12}^3-c_{11}c_{12}^2\right)\left(c_{11}^2-c_{12}^2\right)^{-1}, \quad \delta_1^{11(p)}=\delta_1^{11(r)}=0, \tag{7.21}$$

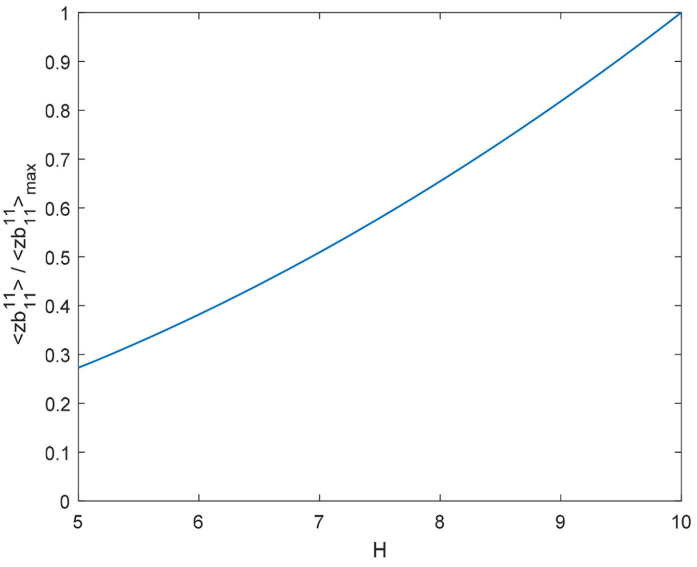

Figure 6. Plot of the effective coupling elastic coefficient $\langle zb_{11}^{11} \rangle$ vs. height of the GaAs rib for the ribbed plate of Figure 5.

where the superscripts p and r denote the plate and rib, respectively. It should be noted that the expression for b_{11}^{11} in the region of the rib is equivalent to the stiffness modulus (Young's Modulus) of the material of the rib (in the x_1 direction) and that these results match the corresponding expressions obtained in Hadjiloizi et al. [51,55]. The effective extensional, $\langle b_{11}^{11} \rangle$, and coupling, $\langle zb_{11}^{11} \rangle$, coefficients are determined from equations (7.21) and (3.12) and are given by,

$$\langle b_{11}^{11} \rangle = b_{11}^{11(p)} + b_{11}^{11(r)} \left(\frac{Ht_2}{h_2} \right), \quad \langle zb_{11}^{11} \rangle = b_{11}^{11(r)} \left(H^2 + H \right) \frac{t_2}{2h_2}. \tag{7.22}$$

The calculation of the remaining effective properties coming from equation (7.18a) as well as the solution of the other two unit cell problems in equation (4.7) follow along the same lines and will not be shown here. As a simple example, Figure 6 shows the variation of $\langle zb_{11}^{11} \rangle$ vs. the height of the rib for a ribbed structure made of a $BaTiO_3$ base plate and a GaAs rib with $t_2/h_2 = 0.1$ and properties given in Guinovart-Sanjuán et al. [24]. The stiffening effect produced by increasing the height of the rib is evident in Figure 6. Much like the previous example pertaining to the laminated structure, this plot highlights the flexibility of the developed model to accommodate a broad range of architectures and tailor the effective properties of a given structure according to the requirements of a particular application by changing various parameters (geometrical, physical, material) as needed. We finally note that the results for the effective elastic coefficients (extensional, bending and coupling) for the ribbed plate, agree very closely with the corresponding results known from the structurally anisotropic theory of strengthened plates and shells, with the exception of the $\langle zB_{12}^{*12} \rangle$ coefficient (effective torsional stiffness) [49].

It is important at this point to provide a few details on the limits of applicability and range of accuracy of the developed model. To this end, we note that the homogenization problem for periodically inhomogeneous thin plates was first addressed by Duvaut and Metellus [75] and Artola and Duvaut [76]. In those works, the expressions for the effective coefficients obtained were valid only for plates whose thickness was much smaller than the length of the period of the inhomogeneity, i.e., the unit cell. This assumption is not always valid or realizable however, and it is often the case that the thickness of the plate and the length of the period are of comparable order of magnitude. Based on this premise and the early works of Caillerie [77,78], a significant number of works pertaining to the asymptotic homogenization modeling and analysis of inhomogeneous thin-walled structures was disseminated. For a more detailed mathematical analysis, the reader is referred to Caillerie [77,78]. The model developed and illustrated in the present manuscript is based on this assumption and, as we have seen, employs two

microscopic variables, one in the tangential directions characterized by periodicity and one in the transverse direction in which no periodicity exists.

Pertaining to the ribbed plate example examined in this section, we note that the approximate solutions of the local problems were obtained under the assumption that the thickness of each element was smaller than the other two dimensions, see Kalamkarov [49], and we also ignored stress concentrations and other complications at the joint regions between the ribs and the plates. Essentially, these regions are highly localized and do not contribute significantly to the integrals over the volume of the unit cell. A more refined analysis (first-gradient homogenization only) where these stress concentrations are taken into account via the introduction of appropriate singularity functions reveals that the error incurred by ignoring them is fairly small for most effective coefficients, see Kalamkarov [49].

Before closing this section, we reiterate that the general model developed in this work, sections 2–6, is quite general and can be applied to a broad range of composite and reinforced flexoelectric structures beyond those examined in section 7. Furthermore, with the appropriate modifications, the model can also be extended to the analysis of reinforced flexoelectric shells, including geometrically nonlinear shells, to examine quasi-static, dynamic, stability, and other problems. For relevant literature, we refer the readers to the authors' recent works on thin magnetoelectric shells, [42–44], where only first-gradient homogenization is considered (and therefore no flexoelectric behavior is examined), the works of Guinovart-Sanjuán et al. [25,57,59] on thick flexoelectric and other composite shells, as well as earlier works involving dynamic stability of thick cylindrical shells, see, for example, the works of Bert and Birman [79], and Darabi et al. [80]. Another interesting application for which the developed model can be adapted pertains to self-assembled semiconductor quantum dots which can be encouraged to grow at periodic locations by pre-patterning of the substrate [81]. In a similar direction, we note the recent publication of the first author and collaborators pertaining to the development of a 3D, first-gradient asymptotic homogenization model on quantum-dot embedded nanocomposite materials [82].

Conclusion

A micromechanical model for the analysis of structurally periodic flexoelectric and piezoelectric plates with rapidly varying thickness is developed on the basis of asymptotic homogenization. The model successfully decouples the microscopic and the macroscopic scales so that they are handled separately and independently of one another. The microscopic problem is implemented in two steps, one pertaining to first-gradient asymptotic homogenization and the other to second-gradient asymptotic homogenization involving the second gradient of mechanical displacement and electric potential. The two homogenization steps generate a total of 10 unit cell problems that eventually yield the effective coefficients of the homogenized flexoelectric plate. Once these are determined, they enter a set of governing equations (macroscopic problem) which permit the evaluation of macroscopic displacement and electric potential. The desired field variables of mechanical stress, electric displacement, mechanical strain and its gradient, electric field and its gradient, and so on can finally be obtained via asymptotic approximations.

One interesting feature of the developed model is its flexibility which renders it applicable to a broad range of geometries including both stratified flexoelectric structures as well as reinforced flexoelectric plates with a periodic arrangement of reinforcements attached to the bottom and top surfaces. Furthermore, the closed-form expressions for the effective properties allow for their customization to the requirements of a particular application by changing various geometric, physical, or material parameters of interest. Another interesting feature of the developed model is that it pertains to flexoelectric structures with distinct in-plane and out-of-plane behavior (such as bending and torsion) whereby periodicity exists in the tangential directions only. Thus, the presented model complements earlier published works pertaining, primarily, to 3D structures which essentially used a 3D formalism with periodicity in all three spatial directions.

The present work is illustrated by means of laminated flexoelectric composites as well as simple rib-reinforced plates. The solution methodology for the unit cell problems is shown and the local coefficients, coefficient functions, and effective coefficients are determined. Finally, it is shown that in the limiting case of a thin, purely elastic plate, the derived model converges to the familiar classical plate model.

Funding

The author(s) disclosed receipt of the following financial support for the research, authorship, and/or publication of this article: The authors would like to acknowledge the financial support of the Natural Sciences and Engineering Research Council of Canada (NSERC Grant # RGPIN-2020-03899, first author), the Science Foundation Ireland (SFI) for funding Spatially and Temporally VARIable COMPosite Structures (VARICOMP) Grant No. (15/RP/2773) under its Research Professor program (second and third authors), and the Cyprus University of Technology and the Research Unit for Nanostructured Materials Systems (fourth author).

ORCID iD

AV Georgiades https://orcid.org/0000-0002-8984-1011

References

[1] Sevostianov, I. On the thermal expansion of composite materials and cross-property connection between thermal expansion and thermal conductivity. *Mech Mater* 2011; 45: 20–33.
[2] Sevostianov, I, and Kachanov, M. Connections between elastic and conductive properties of heterogeneous materials. *Adv Appl Mech* 2009; 42: 69–253.
[3] Sevostianov, I, and Kachanov, M. On the possibility to represent effective properties of a material with inhomogeneities in terms of a single concentration parameter. *Int J Solids Struct* 2015; 52: 197–204.
[4] Sevostianov, I, and Kachanov, M. On some controversial issues in theories of effective properties. *Mech Mater* 2014; 69: 93–105.
[5] Sevostianov, I, and Giraud, A. Generalization of Maxwell homogenization scheme for elastic material containing inhomogeneities of diverse shape. *Int J Eng Sci* 2013; 64: 23–36.
[6] Guo, J, Gallegos, JJ, Tom, AR, et al. Electric-field-guided precision manipulation of catalytic nanomotors for cargo delivery and powering nanoelectromechanical devices. *ACS Nano* 2018; 12: 1179–1187.
[7] Wang, L, and Wang, ZL. Advances in piezotronics transistors and piezotronics. *Nano Today* 2021; 37: 101108.
[8] Benoit, RR, Rudy, RQ, Pulskamp, JS, et al. Piezoelectric RF MEMS switches on Si-on-Sapphire substrates. *J Micromech Syst* 2020; 29(5): 1087–1090.
[9] Saya, D, Dezest, D, Welsh, AJ, et al. Piezoelectric nanoelectromechanical systems integrating microcontact printed lead zirconium titanate films. *J Micromech Microeng* 2020; 30: 035004.
[10] Falconi, C. Piezoelectric nanotransducers. *Nanoenergy* 2019; 59: 730–744.
[11] Guo, S, Duan, X, Xie, M, et al. Composites, fabrication and application of polyvinylidene fluoride for flexible electromechanical devices: a review. *Micromachines* 2020; 11: 1076.
[12] Maranganti, R, Sharma, ND, and Sharma, P. Electromechanical coupling in nonpiezoelectric materials due to nanoscale nonlocal effects: green's function solutions and embedded inclusions. *Phys Rev B* 2006; 74: 014110.
[13] Sharma, ND, Maranganti, R, and Sharma, P. On the possibility of piezoelectric nanocomposites without using piezoelectric materials. *J Mech Phys Solids* 2007; 55: 2328–2350.
[14] Sharma, ND, Landis, CM, and Sharma, P. Piezoelectric thin-film superlattices without using piezoelectric materials. *J Appl Phys* 2010; 108: 024304.
[15] Shu, L, Liang, R, Rao, Z, et al. Flexoelectric materials and their related applications: a focused review. *J Adv Ceram* 2019; 8(2): 153–173.
[16] Huang, S, Qi, L, Huang, W, et al. Flexoelectricity in dielectrics: materials, structures and characterizations. *J Adv Dielectr* 2018; 8(2): 183002.
[17] Liang, X, Hu, S, and Shen, S. Nanoscale mechanical energy harvesting using piezoelectricity and flexoelectricity. *Smart Mater Struct* 2017; 26: 035050.
[18] Gilroy, C, McKay, K, Devine, M, et al. Active chiral plasmonics: flexoelectric control of nanoscale chirality. *Adv Photonics Res* 2021; 2: 2000062.
[19] Yudin, PV, and Tagantsev, AK. Fundamentals of flexoelectricity in solids. *Nanotechnology* 2014; 24: 432001.
[20] Mindlin, RD. Second gradient of strain and surface-tension in linear elasticity. *Int J Solids Struct* 1965; 1: 417–438.
[21] Ghasemi, H, Park, HS, and Rabczuk, T. A multi material level set-based topology optimization of flexoelectric composites. *Comput Methods Appl Mech Eng* 2018; 332: 47–62.
[22] Hamdia, KM, Ghasemi, H, Zhuang, X, et al. Multilevel Monte Carlo method for topology optimization of flexoelectric composites with uncertain material properties. *Eng Anal Bound Elem* 2022; 134: 412–418.
[23] Chen, X, Yvonnet, J, Yao, S, et al. Topology optimization of flexoelectric composites using computational homogenization. *Comput Methods Appl Mech Eng* 2021; 381: 113819.
[24] Guinovart-Sanjuán, D, Vajravelu, K, Rodríguez-Ramos, R, et al. Simple closed-form expressions for the effective properties of multilaminated flexoelectric composites. *J Eng Math* 2021; 127: 4.

[25] Guinovart-Sanjuán, D, Vajravelu, K, Rodríguez-Ramos, R, et al. Effective predictions of heterogeneous flexoelectric multilayered composite with generalized periodicity. *Int J Mech Sci* 2020; 181: 105755.
[26] Nasimsobhan, M, Ganghoffer, J-F, and Shamshirsaz, M. Construction of piezoelectric and flexoelectric models of composites by asymptotic homogenization and application to laminates. *Math Mech Solids* 2022; 27(4): 602–637.
[27] Zheng, Y, Chu, L, Dui, G, et al. Numerical predictions for the effective electrical properties of flexoelectric composites with a single inclusion. *Appl Phys A* 2021; 127: 686.
[28] Mawassy, N, Reda, H, Ganghoffer, J-F, et al. A variational approach of homogenization of piezoelectric composites towards piezoelectric and flexoelectric effective media. *Int J Eng Sci* 2021; 158: 103410.
[29] Yang, H, Abali, BE, Timofeev, D, et al. Determination of metamaterial parameters by means of a homogenization approach based on asymptotic analysis. *Continuum Mech Therm* 2020; 32: 1251–1270.
[30] Chu, L, Dui, G, and Ju, C. Flexoelectric effect on the bending and vibration responses of functionally graded piezoelectric nanobeams based on general modified strain gradient theory. *Compos Struct* 2018; 186: 39–49.
[31] Chen, W, Liang, X, and Shen, S. Forced vibration of piezoelectric and flexoelectric Euler-Bernoulli beams by dynamic Green's functions. *Acta Mech* 2020; 232: 449–460.
[32] Yan, Z, and Jiang, L. Size-dependent bending and vibration behavior of piezoelectric nanobeams due to flexoelectricity. *J Phys D Appl Phys* 2013; 46: 355502.
[33] Zhao, X, Zheng, S, and Li, Z. Size-dependent nonlinear bending and vibration of flexoelectric nanobeam based on strain gradient theory. *Smart Mater Struct* 2019; 28: 75027.
[34] Kundalwal, SI, and Shingare, KB. Electromechanical response of thin shell laminated with flexoelectric composite layer. *Thin-Walled Struct* 2020; 157: 107138.
[35] Shingare, KB, and Naskar, S. Analytical solution for static and dynamic analysis of graphene-based hybrid flexoelectric nanostructures. *J Compos Sci* 2021; 5: 74.
[36] Mu, F, Zhongmin, X, and Hornsen, T. Distributed multi-flexoelectric actuation and control of plates. *AIAAJ* 2020; 58: 1377–1385.
[37] Chen, L, Pan, S, Fei, Y, et al. Theoretical study of micro/nano-scale bistable plate for flexoelectric energy harvesting. *Appl Phys A* 2019; 125: 24.
[38] Wang, B, and Li, X-F. Flexoelectric effects on the natural frequencies for free vibration of piezoelectric nanoplates. *J Appl Phys* 2021; 129: 034102.
[39] Hadjiloizi, DA, Kalamkarov, AL, and Georgiades, AV. Micromechanical analysis of piezo-magneto-thermo-elastic T-ribbed and Π-ribbed plates. *Mech Adv Mater Struct* 2018; 25(8): 657–668.
[40] Hadjiloizi, DA, Kalamkarov, AL, Saha, GC, et al. Micromechanical modeling of thin composite and reinforced magnetoelectric plates—effective elastic, piezoelectric and piezomagnetic coefficients. *Compos Struct* 2017; 172: 102–118.
[41] Hadjiloizi, DA, Kalamkarov, AL, Saha, GC, et al. Micromechanical modeling of thin composite and reinforced magnetoelectric plates—effective electrical, magnetic, thermal and product properties. *Compos Part B Eng* 2017; 113: 243–269.
[42] Christofi, I, Hadjiloizi, DA, Kalamkarov, AL, et al. Asymptotic homogenization of magnetoelectric reinforced shells: Effective coefficients and influence of shell curvature. *Int J Solids Struct* 2021; 228: 111105.
[43] Christofi, I, Hadjiloizi, DA, Kalamkarov, AL, et al. Micromechanical analysis of thermoelastic and magnetoelectric composite and reinforced shells. *Compos Struct* 2021; 259: 113426.
[44] Christofi, I, Hadjiloizi, DA, Kalamkarov, AL, et al. Dynamic micromechanical model for smart composite and reinforced shells. *ZAMM J Appl Math Mech* 2022; 102: e202100211.
[45] Bensoussan, A, Lions, JL, and Papanicolaou, G. *Asymptotic analysis for periodic structures*. Amsterdam, NY: North-Holland, 1978.
[46] Sanchez-Palencia, E. *Non-homogeneous media and vibration theory*. Berlin: Springer-Verlag, 1980.
[47] Bakhvalov, N, and Panasenko, G. *Homogenisation: averaging processes in periodic media*. Amsterdam, NY: Kluwer Academic Publishers, 1984.
[48] Cioranescu, D, and Donato, P. *An introduction to homogenization*. Oxford: Oxford University Press, 1999.
[49] Kalamkarov, AL. *Composite and reinforced elements of construction*. New York: Wiley, 1992.
[50] Kalamkarov, AL, and Kolpakov, AG. *Analysis, design and optimization of composite structures*. New York: Wiley, 1997.
[51] Hadjiloizi, DA, Kalamkarov, AL, Metti, C, et al. Analysis of smart piezo-magneto-thermo-elastic composite and reinforced plates: part I-model development. *Curved Layer Struct* 2014; 1: 11–31.
[52] Hadjiloizi, DA, and Weaver, PM. Asymptotic homogenization for modeling of wingbox structures. In: *2018 AIAA/ASCE/AHS/ASC structures, structural dynamics, and materials conference*, Kissimmee, FL, USA, 8–12 January 2018, pp.0477. Reston, VA: American Institute of Aeronautics and Astronautics.
[53] Hadjiloizi, DA, Georgiades, AV, and Kalamkarov, AL. Dynamic modeling and determination of effective properties of smart composite plates with rapidly varying thickness. *Int J Eng Sci* 2012; 56: 63–85.
[54] Hadjiloizi, DA, Kalamkarov, AL, and Georgiades, AV. Plane stress analysis of magnetoelectric composite and reinforced plates: Micromechanical modeling and application to laminated structures. *Z Angew Math Mech* 2017; 97: 761–785.

[55] Hadjiloizi, DA, Kalamkarov, AL, and Georgiades, AV. Plane stress analysis of magnetoelectric composite and reinforced plates: Applications to wafer- and rib-reinforced plates and three-layered honeycomb shells. *Z Angew Math Mech* 2017; 97: 786–814.
[56] Guinovart-Sanjuán, D, Rizzoni, R, Rodríguez-Ramos, R, et al. Assessment of models and methods for pressurized spherical composites. *Math Mech Solids* 2018; 23(2): 136–147.
[57] Guinovart-Sanjuán, D, Rizzoni, R, Rodríguez-Ramos, R, et al. Behavior of laminated shell composite with imperfect contact between the layers. *Compos Struct* 2017; 176: 539–546.
[58] Guinovart-Sanjuán, D, Rodríguez-Ramos, R, Guinovart-Díaz, R, et al. Effective properties of regular elastic laminated shell composite. *Compos Part B* 2016; 82: 12–20.
[59] Guinovart-Sanjuán, D, Vajravelu, K, Rodríguez-Ramos, R, et al. Analysis of effective elastic properties for shells with complex geometrical shapes. *Compos Struct* 2018; *b* 203: 278–285.
[60] Lapeyronnie, P, Le Grognec, P, Binétruy, C, et al. Homogenization of the elastic behavior of a layer-to-layer angle-interlock composite. *Compos Struct* 2011; 93(11): 2795–2807.
[61] Barchiesi, E. Multi-scale and multi-physics: towards next-generation engineering materials. *Continuum Mech Therm* 2020; 32: 541–554.
[62] Estrin, Y, Krishnamurthy, VR, and Akleman, E. Design of architecture materials based on topological and geometrical interlocking. *J Mater Res Technol* 2021; 15: 1165–1178.
[63] Abali, EA, and Barchiesi, E. Additive manufacturing introduced substructure and computational determination of metamaterials parameters by means of asymptotic homogenization. *Continuum Mech Therm* 2021; 33: 993–1049.
[64] Bruggi, M, and Taliercio, A. Hierarchical infills for additive manufacturing through a multiscale approach. *J Optimiz Theory Appl* 2020; 187: 654–682.
[65] De Bellis, ML, Bacigalupo, A, and Zavarise, G. Characterization of hybrid piezoelectric nanogenerators through asymptotic homogenization. *Comput Methods Appl Mech Eng* 2019; 355: 1148–1186.
[66] Del Toro, R, Bacigalupo, A, and Paggi, M. Characterization of wave propagation in periodic viscoelastic materials via asymptotic-variational homogenization. *Int J Solids Struct* 2019; 172-173: 110–146.
[67] Préve, D, Bacigalupo, A, and Paggi, M. Variational-asymptotic homogenization of thermoelastic periodic materials with thermal relaxation. *Int J Mech Sci* 2021; 205: 106566.
[68] Rahali, Y, Eremeyev, VA, and Ganghoffer, JF. Surface effects of network materials based on strain gradient homogenized media. *Math Mech Solids* 2020; 25(2): 389–406.
[69] Hu, S, and Shen, S. Variational principles and governing equations in nano-dielectrics with the flexoelectric effect. *Sci China Phys Mech Astron* 2010; 53: 1497–1504.
[70] Shen, S, and Hu, S. A theory of flexoelectricity with surface effect for elastic dielectrics. *J Mech Phys Solids* 2010; 58: 665–677.
[71] Zhuang, X, Nguyen, BH, Nanthakumar, SS, et al. Computational modeling of flexoelectricity—a review. *Energies* 2020; 13: 1326.
[72] Abdollahi, A, Peco, C, Millán, D, et al. Computational evaluation of the flexoelectric effect in dielectric solids. *J Appl Phys* 2014; 116: 93502.
[73] Gibson, RF. *Principles of composite material mechanics*. New York: McGraw-Hill, 1994.
[74] Reddy, JN. *Mechanics of laminated composite plates and shells*. New York: CRC Press, 2003.
[75] Duvaut, G, and Metellus, A-M. Homogeneisation d'une plaque mince en flexion de structure periodique et symetrique. *CR Acad Sci Paris Sér A* 1976; 283(13): 947–950.
[76] Artola, M, and Duvaut, G. Homogeneisation d'une plaque renforcee. *CR Acad Sci Paris Sér A* 1977; 284: 707–710.
[77] Caillerie, D. Plaques elastique minces à structure périodique de période et d'épaisseur comparables. *CR Acad Sci Paris Sér II* 1982; 294: 159–162.
[78] Caillerie, D. Thin elastic and periodic plates. *Math Meth Appl Sci* 1984; 6: 159–191.
[79] Bert, CW, and Birman, V. Parametric instability of thick, orthotropic, circular cylindrical shells. *Acta Mechanica* 1988; 71: 61–76.
[80] Darabi, M, Darvizeh, M, and Darvizeh, A. Non-linear analysis of dynamic stability for functionally graded cylindrical shells under periodic axial loading. *Compos Struct* 2008; 83: 201–211.
[81] Warburton, RJ. Self-assembled semiconductor quantum dots. *Contemp Phys* 2002; 43(5): 351–364.
[82] Alam, A, Saha, GC, and Kalamkarov, AL. Micromechanical analysis of quantum dot-embedded smart nanocomposite materials. *Compos Part C* 2020; 3: 100062.

Appendix A: Definitions of variables and differential operators

The differential operators appearing in equations (4.5a) and (4.5b) as well as their counterparts in equations (4.14a) and (4.14b) are defined in equations (A.1) and (A.2) below:

$$
\begin{aligned}
&L_{ijk}=c_{ijk\mu}\frac{1}{h_\mu}\frac{\partial}{\partial y_\mu}+c_{ijk3}\frac{\partial}{\partial z},\quad M_{ij}=e_{\mu ij}\frac{1}{h_\mu}\frac{\partial}{\partial y_\mu}+e_{3ij}\frac{\partial}{\partial z},\quad D_{ik}=\frac{1}{h_\mu}\frac{\partial}{\partial y_\mu}L_{i\mu k}+\frac{\partial}{\partial z}L_{i3k}\\
&C_i=\frac{1}{h_\mu}\frac{\partial}{\partial y_\mu}M_{i\mu}+\frac{\partial}{\partial z}M_{i3},\quad C_{ik\lambda}=\frac{1}{h_\mu}\frac{\partial c_{i\mu k\lambda}}{\partial y_\mu}+\frac{\partial c_{i3k\lambda}}{\partial z},\quad P_{\lambda i}=\frac{1}{h_\mu}\frac{\partial e_{\lambda i\mu}}{\partial y_\mu}+\frac{\partial e_{\lambda i3}}{\partial z}\\
&L^*_{ik}=e_{ik\mu}\frac{1}{h_\mu}\frac{\partial}{\partial y_\mu}+e_{ik3}\frac{\partial}{\partial z},\quad M^*_i=\kappa_{i\mu}\frac{1}{h_\mu}\frac{\partial}{\partial y_\mu}+\kappa_{i3}\frac{\partial}{\partial z},\quad A^*_i=\frac{1}{h_\mu}\frac{\partial}{\partial y_\mu}L^*_{\mu k}+\frac{\partial}{\partial z}L^*_{3k}\\
&L^*=\frac{1}{h_\mu}\frac{\partial}{\partial y_\mu}M^*_\mu+\frac{\partial}{\partial z}M^*_3,\quad G^*_{k\lambda}=\frac{1}{h_\mu}\frac{\partial e_{\mu k\lambda}}{\partial y_\mu}+\frac{\partial e_{3k\lambda}}{\partial z},\quad I^*_\lambda=\frac{1}{h_\mu}\frac{\partial \kappa_{\mu\lambda}}{\partial y_\mu}+\frac{\partial \kappa_{3\lambda}}{\partial z}.
\end{aligned}
\tag{A.1}
$$

$$
\begin{aligned}
&M^{(2)}_{ij}=-\mu^{(f)}_{\alpha ij\beta}\frac{1}{h_\alpha h_\beta}\frac{\partial^2}{\partial y_\alpha\partial y_\beta}-\left[\mu^{(f)}_{3ij\beta}+\mu^{(f)}_{\beta ij3}\right]\frac{1}{h_\beta}\frac{\partial^2}{\partial z\partial y_\beta}-\mu^{(f)}_{3ij3}\frac{\partial^2}{\partial z^2},\quad M^{(2)(f)}_{ij}=M_{ij}+M^{(2)}_{ij}\\
&N^*_{ij}=\mu^{(f)}_{ij\alpha\beta}\frac{1}{h_\alpha h_\beta}\frac{\partial^2}{\partial y_\alpha\partial y_\beta}+\left[\mu^{(f)}_{ij3\beta}+\mu^{(f)}_{ij\beta3}\right]\frac{1}{h_\beta}\frac{\partial^2}{\partial z\partial y_\beta}+\mu^{(f)}_{ij33}\frac{\partial^2}{\partial z^2},\quad L^{*(2)}_{ik}=L^*_{ik}+N^*_{ik}\\
&L^{(4)}_{ik}=D_{ik}=\frac{1}{h_\alpha}\frac{\partial}{\partial y_\alpha}L_{i\alpha k}+\frac{\partial}{\partial z}L_{i3k},\quad \tilde\tau^{(4)}_k=\frac{1}{h_\alpha}\frac{\partial}{\partial y_\alpha}L^{*(2)}_{\alpha k}+\frac{\partial}{\partial z}L^{*(2)}_{3k}\\
&\tilde\tau^{(4)}=\frac{1}{h_\alpha}\frac{\partial}{\partial y_\alpha}M^*_\alpha+\frac{\partial}{\partial z}M^*_3,\quad \tilde\mu^{(3)}_{\alpha\beta k}=\frac{1}{h_\nu}\frac{\partial}{\partial y_\nu}\mu^{(f)}_{\nu\alpha\beta k}+\frac{\partial}{\partial z}\mu^{(f)}_{3\alpha\beta k}.
\end{aligned}
\tag{A.2}
$$

The microscopic variables appearing in equations (5.1a)–(5.1d) are defined in equations (A.3)–(A5) below, with δ_{ij} representing Kronecker delta:

$$
\begin{aligned}
&A^{\mu\nu\lambda}_{\alpha\beta}=\frac{1}{2}\left(N^{(1)\mu\nu}_{\alpha}\delta_{\beta\lambda}+N^{(1)\mu\nu}_{\beta}\delta_{\alpha\lambda}\right),\quad A^{\mu\nu\lambda}_{3\beta}=N^{(1)\mu\nu}_{3}\delta_{\beta\lambda},\quad \Gamma^{\nu\lambda}_{\alpha\beta}=\frac{1}{2}\left(M^{(1)\nu}_{\alpha}\delta_{\beta\lambda}+M^{(1)\nu}_{\beta}\delta_{\alpha\lambda}\right)\\
&\Delta^{\mu\nu\lambda}_{\alpha\beta\gamma}=\frac{1}{2}\left(\delta_{\alpha\mu}\delta_{\gamma\mu}\delta_{\beta\lambda}+\delta_{\beta\mu}\delta_{\gamma\nu}\delta_{\alpha\lambda}+h^{-1}_{\beta}N^{(1)\mu\nu}_{\alpha|\beta}\delta_{\gamma\lambda}+h^{-1}_{\alpha}N^{(1)\mu\nu}_{\beta|\alpha}\delta_{\gamma\lambda}+h^{-1}_{\gamma}N^{(1)\mu\nu}_{\alpha|\gamma}\delta_{\beta\lambda}+h^{-1}_{\gamma}N^{(1)\mu\nu}_{\beta|\gamma}\delta_{\alpha\lambda}\right)\\
&\Delta^{\mu\nu\lambda}_{3\beta\gamma}=\left(h^{-1}_{\beta}N^{(1)\mu\nu}_{3|\beta}\delta_{\gamma\lambda}+N^{(1)\mu\nu}_{\beta|3}\delta_{\gamma\lambda}+h^{-1}_{\gamma}N^{(1)\mu\nu}_{3|\gamma}\delta_{\beta\lambda}\right),\quad \Delta^{\mu\nu\lambda}_{\alpha\beta3}=\frac{1}{2}\left(N^{(1)\mu\nu}_{\alpha|3}\delta_{\beta\lambda}+N^{(1)\mu\nu}_{\beta|3}\delta_{\alpha\lambda}\right)\\
&\Delta^{\mu\nu\lambda}_{33\gamma}=N^{(1)\mu\nu}_{3|3}\delta_{\gamma\lambda},\quad \Delta^{\mu\nu\lambda}_{3\beta3}=N^{(1)\mu\nu}_{3|3}\delta_{\beta\lambda},\quad \Gamma^{\nu\lambda}_{3\beta}=M^{(1)\nu}_{3}\delta_{\beta\lambda}.
\end{aligned}
\tag{A.3}
$$

$$
\begin{aligned}
&A^{\mu\nu\lambda}_{\alpha\beta}=\frac{1}{2}\left(N^{(1)\mu\nu}_{\alpha}\delta_{\beta\lambda}+N^{(1)\mu\nu}_{\beta}\delta_{\alpha\lambda}\right),\quad A^{\mu\nu\lambda}_{3\beta}=N^{(1)\mu\nu}_{3}\delta_{\beta\lambda},\quad \Gamma^{\nu\lambda}_{\alpha\beta}=\frac{1}{2}\left(M^{(1)\nu}_{\alpha}\delta_{\beta\lambda}+M^{(1)\nu}_{\beta}\delta_{\alpha\lambda}\right)\\
&\Delta^{\mu\nu\lambda}_{\alpha\beta\gamma}=\frac{1}{2}\left(\delta_{\alpha\mu}\delta_{\gamma\mu}\delta_{\beta\lambda}+\delta_{\beta\mu}\delta_{\gamma\nu}\delta_{\alpha\lambda}+h^{-1}_{\beta}N^{(1)\mu\nu}_{\alpha|\beta}\delta_{\gamma\lambda}+h^{-1}_{\alpha}N^{(1)\mu\nu}_{\beta|\alpha}\delta_{\gamma\lambda}+h^{-1}_{\gamma}N^{(1)\mu\nu}_{\alpha|\gamma}\delta_{\beta\lambda}+h^{-1}_{\gamma}N^{(1)\mu\nu}_{\beta|\gamma}\delta_{\alpha\lambda}\right)\\
&\Delta^{\mu\nu\lambda}_{3\beta\gamma}=\left(h^{-1}_{\beta}N^{(1)\mu\nu}_{3|\beta}\delta_{\gamma\lambda}+N^{(1)\mu\nu}_{\beta|3}\delta_{\gamma\lambda}+h^{-1}_{\gamma}N^{(1)\mu\nu}_{3|\gamma}\delta_{\beta\lambda}\right),\quad \Delta^{\mu\nu\lambda}_{\alpha\beta3}=\frac{1}{2}\left(N^{(1)\mu\nu}_{\alpha|3}\delta_{\beta\lambda}+N^{(1)\mu\nu}_{\beta|3}\delta_{\alpha\lambda}\right)\\
&\Delta^{\mu\nu\lambda}_{33\gamma}=N^{(1)\mu\nu}_{3|3}\delta_{\gamma\lambda},\quad \Delta^{\mu\nu\lambda}_{3\beta3}=N^{(1)\mu\nu}_{3|3}\delta_{\beta\lambda},\quad \Gamma^{\nu\lambda}_{3\beta}=M^{(1)\nu}_{3}\delta_{\beta\lambda}\\
&E^{\nu\lambda}_{\alpha\beta\gamma}=\frac{1}{2}\left(h^{-1}_{\beta}M^{(1)\nu}_{\alpha|\beta}\delta_{\gamma\lambda}+h^{-1}_{\alpha}M^{(1)\nu}_{\beta|\alpha}\delta_{\gamma\lambda}+h^{-1}_{\gamma}M^{(1)\nu}_{\alpha|\gamma}\delta_{\beta\lambda}+h^{-1}_{\gamma}M^{(1)\nu}_{\beta|\gamma}\delta_{\alpha\lambda}\right)\\
&E^{\nu\lambda}_{3\beta\gamma}=\left(h^{-1}_{\beta}M^{(1)\nu}_{3|\beta}\delta_{\gamma\lambda}+M^{(1)\nu}_{\beta|3}\delta_{\gamma\lambda}+h^{-1}_{\gamma}M^{(1)\nu}_{3|\gamma}\delta_{\beta\lambda}\right),\quad E^{\nu\lambda}_{\alpha\beta3}=\frac{1}{2}\left(M^{(1)\nu}_{\alpha|3}\delta_{\beta\lambda}+M^{(1)\nu}_{\beta|3}\delta_{\alpha\lambda}\right)\\
&E^{\nu\lambda}_{33\gamma}=M^{(1)\nu}_{3|3}\delta_{\gamma\lambda},\quad E^{\nu\lambda}_{3\beta3}=M^{(1)\nu}_{3|3}\delta_{\beta\lambda}.
\end{aligned}
\tag{A.4}
$$

$$
\begin{aligned}
&I^{\mu\nu\lambda}_{\beta}=-A^{(1)\mu\nu}\delta_{\beta\lambda},\quad J^{\nu\lambda}_{\beta}=-\Xi^{(1)\nu}\delta_{\beta\lambda},\quad H^{\mu\nu\lambda}_{3\beta}=-A^{(1)\mu\nu}_{|3}\delta_{\beta\lambda}\\
&Z^{\nu\lambda}_{3\beta}=-\Xi^{(1)\nu}_{|3}\delta_{\beta\lambda},\quad H^{\mu\nu\lambda}_{\alpha\beta}=-h^{-1}_{\alpha}A^{(1)\mu\nu}_{|\alpha}\delta_{\beta\lambda}-h^{-1}_{\beta}A^{(1)\mu\nu}_{|\beta}\delta_{\alpha\lambda}\\
&Z^{\nu\lambda}_{\alpha\beta}=\left(-\frac{1}{2}\delta_{\alpha\lambda}\delta_{\beta\nu}-\frac{1}{2}\delta_{\beta\lambda}\delta_{\alpha\nu}-h^{-1}_{\alpha}\Xi^{(1)\nu}_{|\alpha}\delta_{\beta\lambda}-h^{-1}_{\beta}\Xi^{(1)\nu}_{|\beta}\delta_{\alpha\lambda}\right).
\end{aligned}
\tag{A.5}
$$

The microscopic variables and differential operators appearing in equation (5.1e) are defined in equations (A.6) and (A.7) below:

$$\begin{aligned}
&C_{ij}^{\mu\nu\lambda} = c_{ij\alpha\beta}A_{\alpha\beta}^{\mu\nu\lambda} + c_{ij3\beta}A_{3\beta}^{\mu\nu\lambda}, \quad e_{ij}^{\mu\nu\lambda} = -\,e_{\beta ij}I_{\beta}^{\mu\nu\lambda}, \quad d_{ij}^{\mu\nu\lambda} = \mu_{\alpha ij\beta}^{(f)}H_{\alpha\beta}^{\mu\nu\lambda} + \left(\mu_{3ij\beta}^{(f)} + \mu_{\beta ij3}^{(f)}\right)H_{3\beta}^{\mu\nu\lambda} \\
&C_{ij}^{(2)\nu\lambda} = c_{ij\alpha\beta}\Gamma_{\alpha\beta}^{\nu\lambda} + c_{ij3\beta}\Gamma_{3\beta}^{\nu\lambda}, \quad e_{ij}^{(2)\nu\lambda} = -\,e_{\beta ij}J_{\beta}^{\nu\lambda}, \quad d_{ij}^{(2)\nu\lambda} = \mu_{\alpha ij\beta}^{(f)}Z_{\alpha\beta}^{\nu\lambda} + \left(\mu_{3ij\beta}^{(f)} + \mu_{\beta ij3}^{(f)}\right)Z_{3\beta}^{\nu\lambda} \\
&\tilde{b}_{ij}^{\mu\nu\lambda} = C_{ij}^{\mu\nu\lambda} + e_{ij}^{\mu\nu\lambda} + d_{ij}^{\mu\nu\lambda}, \quad \tilde{b}_{ij}^{\nu\lambda} = C_{ij}^{(2)\nu\lambda} + e_{ij}^{(2)\nu\lambda} + d_{ij}^{(2)\nu\lambda}.
\end{aligned} \tag{A.6}$$

$$\begin{aligned}
&\varepsilon_{i}^{\mu\nu\lambda} = e_{i\alpha\beta}A_{\alpha\beta}^{\mu\nu\lambda} + e_{i3\beta}A_{3\beta}^{\mu\nu\lambda}, \quad \varepsilon_{ij}^{(2)\nu\lambda} = e_{i\alpha\beta}\Gamma_{\alpha\beta}^{\nu\lambda} + e_{i3\beta}\Gamma_{3\beta}^{\nu\lambda}, \quad \kappa_{i}^{\mu\nu\lambda} = \kappa_{i\beta}I_{\beta}^{\mu\nu\lambda}, \quad \kappa_{i}^{(2)\nu\lambda} = \kappa_{i\beta}J_{\beta}^{\nu\lambda} \\
&f_{i}^{\mu\nu\lambda} = \mu_{i\alpha\beta\gamma}^{(f)}\Delta_{\alpha\beta\gamma}^{\mu\nu\lambda} + \mu_{i3\beta\gamma}^{(f)}\Delta_{3\beta\gamma}^{\mu\nu\lambda} + \mu_{i33\gamma}^{(f)}\Delta_{33\gamma}^{\mu\nu\lambda} + \mu_{i\alpha\beta3}^{(f)}\Delta_{\alpha\beta3}^{\mu\nu\lambda} + \mu_{i3\beta3}^{(f)}\Delta_{3\beta3}^{\mu\nu\lambda} \\
&f_{i}^{(1)\nu\lambda} = \mu_{i\alpha\beta\gamma}^{(f)}E_{\alpha\beta\gamma}^{\nu\lambda} + \mu_{i3\beta\gamma}^{(f)}E_{3\beta\gamma}^{\nu\lambda} + \mu_{i33\gamma}^{(f)}E_{33\gamma}^{\nu\lambda} + \mu_{i\alpha\beta3}^{(f)}E_{\alpha\beta3}^{\nu\lambda} + \mu_{i3\beta3}^{(f)}E_{3\beta3}^{\nu\lambda} \\
&\tilde{\delta}_{i}^{\mu\nu\lambda} = \varepsilon_{i}^{\mu\nu\lambda} + \kappa_{i}^{\mu\nu\lambda} + f_{i}^{\mu\nu\lambda}, \quad \tilde{\delta}_{i}^{(2)\nu\lambda} = \varepsilon_{ij}^{(2)\nu\lambda} + \kappa_{i}^{(2)\nu\lambda} + f_{i}^{(1)\nu\lambda}
\end{aligned} \tag{A.7}$$

The microscopic variables and differential operators appearing in equations (5.4a) and (5.4b) are defined in equation (A.8) below:

$$\begin{aligned}
&\tilde{b}_{i}^{(3)\mu\nu\lambda} = h_{\gamma}^{-1}\tilde{b}_{i\gamma|\gamma}^{\mu\nu\lambda} + \tilde{b}_{i3|3}^{\mu\nu\lambda}, \quad \tilde{b}_{i}^{(3)\nu\lambda} = h_{\gamma}^{-1}\tilde{b}_{i\gamma|\gamma}^{\nu\lambda} + \tilde{b}_{i3|3}^{\nu\lambda}, \quad \tilde{\sigma}^{(3)\mu\nu\lambda} = h_{\gamma}^{-1}\tilde{\delta}_{\gamma|\gamma}^{\mu\nu\lambda} + \tilde{\delta}_{3|3}^{\mu\nu\lambda} \\
&\tilde{\sigma}^{*(3)\nu\lambda} = h_{\gamma}^{-1}\tilde{\delta}_{\gamma|\gamma}^{(2)\nu\lambda} + \tilde{\delta}_{3|3}^{(2)\nu\lambda}, \quad M_{i}^{(4)} = h_{\gamma}^{-1}M_{i\gamma|\gamma}^{(2)(f)} + L_{i3k|3}.
\end{aligned} \tag{A.8}$$

Appendix B: Material properties for cubic crystal symmetry around x_3 axis

Following [24], we may write down the constitutive relationships of equation (3.2d) in matrix form as:

$$\begin{bmatrix} \boldsymbol{\sigma}_{6\times1} \\ \boldsymbol{D}_{3\times1} \end{bmatrix} = \begin{bmatrix} \boldsymbol{C}_{6\times6} & -\boldsymbol{e}_{6\times3}^{\mathrm{T}} & \boldsymbol{0}_{6\times18} & \boldsymbol{\mu}_{6\times9} \\ \boldsymbol{e}_{3\times6} & \boldsymbol{\kappa}_{3\times3} & \boldsymbol{\mu}_{3\times18} & \boldsymbol{0}_{3\times9} \end{bmatrix} \begin{bmatrix} \boldsymbol{\varepsilon}_{6\times1} \\ \boldsymbol{E}_{3\times1} \\ \nabla\boldsymbol{\varepsilon}_{18\times1} \\ \nabla\boldsymbol{E}_{9\times1} \end{bmatrix}. \tag{B.1}$$

The $\boldsymbol{C}_{6\times6}$, $\boldsymbol{e}_{6\times3}^{\mathrm{T}}$, and $\boldsymbol{\kappa}_{3\times3}$ material sub-matrices appearing in equation (B.1) are given below in compact notation, see Guinovart-Sanjuán et al. [24].

$$\boldsymbol{C}_{6\times6} = \begin{bmatrix} c_{11} & c_{12} & c_{12} & 0 & 0 & 0 \\ c_{12} & c_{11} & c_{12} & 0 & 0 & 0 \\ c_{12} & c_{12} & c_{11} & 0 & 0 & 0 \\ 0 & 0 & 0 & c_{66} & 0 & 0 \\ 0 & 0 & 0 & 0 & c_{66} & 0 \\ 0 & 0 & 0 & 0 & 0 & c_{66} \end{bmatrix}, \quad \boldsymbol{e}_{6\times3}^{\mathrm{T}} = \begin{bmatrix} 0 & 0 & 0 \\ 0 & 0 & 0 \\ 0 & 0 & 0 \\ e_{14} & 0 & 0 \\ 0 & e_{14} & 0 \\ 0 & 0 & e_{14} \end{bmatrix}, \quad \boldsymbol{\kappa}_{3\times3} = \begin{bmatrix} \kappa_{11} & 0 & 0 \\ 0 & \kappa_{11} & 0 \\ 0 & 0 & \kappa_{11} \end{bmatrix}. \tag{B.2}$$

The $\boldsymbol{\mu}_{6\times9}$ sub-matrix is expressed as,

$$\boldsymbol{\mu}_{6\times6} = \begin{bmatrix} \mu_{1111} & \mu_{2111} & \mu_{3111} & \mu_{1112} & \mu_{2112} & \mu_{3112} & \mu_{1113} & \mu_{2113} & \mu_{3113} \\ \mu_{1221} & \mu_{2221} & \mu_{3221} & \mu_{1222} & \mu_{2222} & \mu_{3222} & \mu_{1223} & \mu_{2223} & \mu_{3223} \\ \mu_{1331} & \mu_{2331} & \mu_{3331} & \mu_{1332} & \mu_{2332} & \mu_{3332} & \mu_{1333} & \mu_{2333} & \mu_{3333} \\ \mu_{1231} & \mu_{2231} & \mu_{3231} & \mu_{1232} & \mu_{2232} & \mu_{3232} & \mu_{1233} & \mu_{2233} & \mu_{3233} \\ \mu_{1131} & \mu_{2131} & \mu_{3131} & \mu_{1132} & \mu_{2132} & \mu_{3132} & \mu_{1133} & \mu_{2133} & \mu_{3133} \\ \mu_{1121} & \mu_{2121} & \mu_{3121} & \mu_{1122} & \mu_{2122} & \mu_{3122} & \mu_{1123} & \mu_{2123} & \mu_{3123} \end{bmatrix}. \tag{B.3}$$

so that for the cubic symmetry under investigation this matrix coefficients become,

$$\boldsymbol{\mu}_{6\times 6}=\begin{bmatrix} \mu_{11} & 0 & 0 & 0 & \mu_{15} & 0 & 0 & 0 & \mu_{15} \\ \mu_{15} & 0 & 0 & 0 & \mu_{11} & 0 & 0 & 0 & \mu_{15} \\ \mu_{15} & 0 & 0 & 0 & \mu_{15} & 0 & 0 & 0 & \mu_{11} \\ 0 & 0 & 0 & 0 & 0 & \mu_{46} & 0 & \mu_{46} & 0 \\ 0 & 0 & \mu_{46} & 0 & 0 & 0 & \mu_{46} & 0 & 0 \\ 0 & \mu_{46} & 0 & \mu_{46} & 0 & 0 & 0 & 0 & 0 \end{bmatrix}. \tag{B.4}$$

The remaining sub-matrices appearing in equation (B.1) as well as the manner in which $\boldsymbol{\mu}_{3\times 18}$ can be obtained from $\boldsymbol{\mu}_{6\times 6}$ are detailed in Guinovart-Sanjuán et al. [24].